© <2015>. *This manuscript version is made available under the CC-BY-NC-ND 4.0 license* http://creativecommons.org/licenses/by-nc-nd/4.0/

This document is the Accepted Manuscript version of a Published Work that appeared in final form in Archives of Biochemistry and Biophysics. *To access the final edited and published work see* http://dx.doi.org/10.1016/j.abb.2015.08.020

Blue Copper Proteins: A Rigid Machine for Efficient Electron Transfer, a Flexible Device for Metal Uptake

Sergio Alejo Pérez-Henarejos[a], Luis A. Alcaraz[b] and Antonio Donaire[a,*]

[a]Department of Inorganic Chemistry, Faculty of Chemistry, University of Murcia Campus Universitario de Espinardo, 30100-Murcia. Spain.

[b]Bioarray SL, Alicante. Parque Científico de la UMH. Avda Universidad s/n. 03202 Elche (Alicante). Spain.

* Correspondence to: Antonio Donaire.
E-mail address: adonaire@um.es
Department of Inorganic Chemistry, Faculty of Chemistry, University of Murcia. Campus Universitario de Espinardo, 30100-Murcia. Spain.
Phone: (34) 868884627. Fax: (34) 868884148.

Abstract

Blue copper proteins (BCPs) are small and generally soluble copper-containing proteins which participate in monoelectron transfer processes in biological systems. An overview of their electronic and tertiary structure is detailed here. The well-established entatic/rack-induced mechanism is explained by comparing thermodynamic parameters between the folded (tense) and the unfolded (relaxed) forms of the BCP rusticyanin.

Recently, NMR solution data have shown that the active sites of BCPs in absence of the metal ion, *i.e.* in the apoforms, are flexible in the micro-to-second timescale. The rigidity proposed by the entatic/rack-induced mechanism is an imperative for the holoprotein to perform electron transfer; while the flexibility of the apocupredoxin is necessary to uptake the metal ion from the metallochaperones. These apparently contradictory requirements are discussed in the present work. Finally, the role of azurin and some peptides derived from it in anticancer therapy are also described.

Graphical abstract

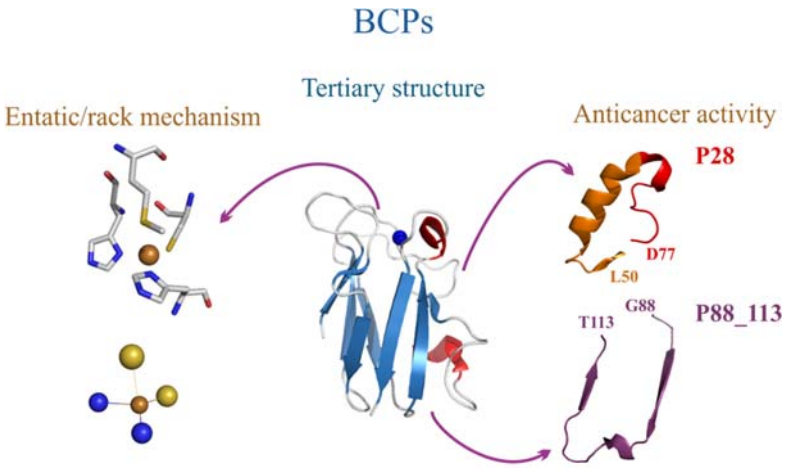

Highlights

- β-barrel in cupredoxins determines the geometry and the electronic structure of the copper ion.
- Holocupredoxins fulfill the entatic/rack-induced mechanism, while apoforms are relaxed.
- Azurin and rusticyanin can be efficient in anticancer and antimalarial therapies.

Keywords

Blue copper proteins, azurin, rusticyanin, rack/entatic, cancer therapy.

Abbreviations

AADH, amine dehydrogenase; Am, amicyanin; Az, azurin; BCPs, Blue Copper Proteins; CPP, cell penetrating peptides; CSP, chemical shift perturbation; EPR, electronic paramagnetic resonance; ET, electron transfer; LMCT, ligand to metal charge transfer; MADH, methylamine dehydrogenase; $MSP1_{19}$, the 19-kDa C-terminal fragment of the *Plasmodium* merozoite surface protein-1; NMR, nuclear magnetic resonance, Pc, plastocyanin; PDB, protein data bank; PSI, phosystem I complex; Rc, rusticyanin; rmsd, root mean squared deviation; ROS, reactive oxidative species; TTQ, tryptophan tryptophylquinone; wt, wild type.

Copper in biological systems

Copper is a first-row transition metal which is essential for life. Although it is only located in low concentration in the Earth crust (*ca*. 60 ppm), it is present in almost all living organisms. The quantity of copper in healthy humans is estimated to be around 100-150 mg. Its deficiency can produce grave illness and, if it is acute, death [1-3].

Copper is very versatile: it can be found in nature with oxidation states I, II or intermediate mixed valences. Since the inter-conversion between the redox states I and II is easily accessible, copper has been chosen by the evolution as one of the two acceptable ions to perform electron transfer (ET) processes (being iron the other chosen one) [4,5]. Copper(II), when combined with oxygen and nitrogen donor atoms, usually becomes soluble and hence, accessible for biological systems. On the contrary, highly insoluble copper(I) has a tendency to coordinate softer donor atoms, such as sulfur. Consequently, when copper(I) combines with these atoms its solubility is extraordinarily increased. Thus, the pair copper(II)/copper(I), and its mixed valence combinations, are optimal candidates to participate in electron transfer processes [6-8]. It is remarkable that copper(I) is a d^{10} ion and so its complexes are diamagnetic and colorless; copper(II), with an uncompleted d^9 shell, provides its complexes with singular spectroscopic features. As a result, most of the knowledge of the electronic structure, and therefore, the function of copper proteins, is due to the studies performed in the paramagnetic oxidized copper(II) form [8,9].

Copper(II) complexes have been classified in different types [10], namely: type 1, type 2, type 3, CuA, CuB and CuZ (Figure 1).

Type 1 or blue copper centers (see Figure 2) give rise to, among others, the Blue Copper Proteins (BCPs), also called cupredoxins, a special set of proteins that are the matter of the present revision. Their features will be extensively commented in the following sections.

Copper type 2, or “normal” copper (Fig. 1A), is extensively found both in the laboratory and in nature. Most type 2 copper centers are three or four coordinated. One or more histidine ligands are always present in copper coordination: three or four imidazol rings are typically found in type 2 sites. Methionine, glutamate, glutamine, tyrosine or even exogenous ligands can complete the coordination sphere. Importantly, non-thiolate groups are coordinated. As a result of this coordination, copper type 2 Uv-

visible absorption spectra are characterized by low intensity *d-d* bands ($\varepsilon \leq 200$ M^{-1} cm^{-1}), while their electron paramagnetic resonance (EPR) spectra display relatively high parallel coupling constants ($A_{\parallel} \geq 140 \times 10^{-4}$ cm^{-1}). This copper is located in multitude of enzymes [10,11] (superoxide dismutase, galactose oxidase, nitrite reductases, copper chaperones as the Atx1-like family, some ATPases…). Copper type 2 is also formed when copper binds to proteins or peptides with still unknown functions: the binding of copper to these proteins normally produces malfunctions and diseases [12], such as: the prion protein [13] (Kreutfeld Jakob or mad cows diseases), XIAP protein [14] (related to the Wilson disease), α-synuclein [15,16] (responsible for the Parkinson disease) or the Aβ-amyloid peptide [17] (Alzheimer's disease). All of them bind copper. This metal seems to accelerate or cause the aggregation of the polypeptide chain, with the subsequent formation of amyloidal plaques and, lastly, the disease.

Type 3 copper (Fig. 1B) is a binuclear center [18,19]. The two copper ions are close (*ca.* 4.0-4.3 Å) and, when oxidized, they are EPR silent due to antiferromagnetic coupling. The absorbance of these ions is also low, as type 2 centers. Hemocyanin or tyrosinase, examples of type 3 copper sites, are related to the biochemistry of dioxygen.

Copper A, CuA (Fig. 1C), consists of two copper ions bridged by two cysteine sulfur atoms [20]. Each copper is also coordinated to a Nδ imidazole atom of a histidine. The sulfur atom of a methionine and the carbonyl oxygen from the backbone complete the tetra-coordination of both copper ions. These centers present a mixed valence state (formally, $Cu^{+1.5}$-$Cu^{+1.5}$) in the oxidized form [21,22]. They are found in several nitrous oxide reductases [23] and in cytochrome *c* oxidases [22].

Copper B, CuB (Fig. 1D), is present in the catalytic center of cytochrome *c* oxidase [24,25]. It consists of a heme a_3, five-coordinated, with a copper ion close to it (*ca.* 5 Å from the iron) and located in trans position with respect to the axial histidine of the iron atom (Figure 1D). The copper ion is coordinated to three histidines, presenting a trigonal pyramidal geometry. The enzyme participates in the reduction of the dioxygen molecule to water.

Copper Z, CuZ (Fig. 1E), is a cluster of four copper ions coordinated to seven histidines. A sulfur atom in the center of the cluster bridges the four ion atoms. This cluster is located in nitrous oxide reductase [26].

Red copper (Fig 1F), which can be found in nitrosocyanin from *Nitrosomonas europaea*, has a histidine and a cysteine as equatorial ligands (similar to copper type 1).

An oxygen atom belonging to the carboxylate group of a glutamate, another histidine and a solvent water molecule complete the metal coordination sphere [27]. The spectroscopic features of this copper site are completely different from those of blue copper sites. In fact, the dominant band appears at 390 nm, providing nitrosocyanin with its characteristic red color; while the EPR spectrum is typical of tetragonal copper [28].

Blue Copper Sites

Architecture of the active sites

Type 1 or blue copper is a mononuclear metal center. Blue copper sites are extensively located in nature, always participating in monoelectron transfer processes. They can be found in large enzymes such as laccases, ascorbate oxidases, nitrite reductases or ceruloplasmins, all of them have molecular weights larger than 60 kDa and contain other metal centers [10]. Blue copper sites can also be found in small (90-160 aa), generally soluble, non-catalytic proteins that act as mediators in electron transfer chains. These are known as Blue Copper Proteins (BCPs). By analogy in the nomenclature, as the small soluble electron transfer iron-sulfur proteins are called ferredoxins, BCPs are also denominated cupredoxins.

The blue copper ion is coordinated to two Nε imidazole nitrogen atoms of two histidines and, strongly, to a Sγ sulfur atom of a cysteine. These four atoms, CuNNS, are tightly bound and are the minimal unit of copper coordination common to all blue copper sites [6,10,29]. A fourth ligand, sited in axial position, typically, but not always, a Sδ sulfur atom of a methionine, can complete the coordination sphere of the copper ion (Figure 2A). However, this axial bound is weaker than the others, as reflected in the Cu-SδMet distance, found between 2.8 and 3.1 Å. This coordination is found in most BCPs, such as plastocyanin, rustycianin, halocyanin, amycianin among others, and also in other blue copper sites such as some nitrite reductases, some lacases, ascorbate oxidases, and ceruloplasmins [10]. In azurins, copper is also weakly coordinated with a backbone carbonyl oxygen located in *trans*-like position in relation to the methionine, so the metal ion can be considered as pentacoordinated (Figure 2B). Instead of a methionine, the axial ligand of stellacyanin is a glutamine, coordinated with the copper ion via the Oε carbonyl atom [30,31] (Figure 2C). Finally, some laccases and

multicopper oxidases do not present an axial coordination, i.e. the copper displays a trigonal geometry [19] (Figure D, no wild-type BCPs are found with this structure).

It is also worth mentioning that a double mutation in azurin copper site takes to the formation of a so-called copper "type zero" [32] (Figure 2E). This is not a wild-type (wt) copper center, in other words, it is not found in nature. Type zero centers have been synthesized in azurin from *Pseudomonas aeruginosa* by simultaneous mutations of the cysteine and the methionine ligands. The cysteine sulfur is substituted by a carboxylate oxygen from an aspartic residue, while the methionine is substituted by a non-ligating amino acid (Leu, Phe or Ile), forcing the metal to attach to the carbonyl glycine in a tetrahedral conformation. Despite the fact that copper in type zero sites does not present a Cu-SγCys bond (there is no cysteine in the coordination sphere), these sites present spectroscopic, redox and kinetics properties similar to those of type 1 sites (see below).

The CuNNS set of atoms are coplanar in laccases and azurins, while the metal ion is outside the NNS plane, pointing towards the axial ligand in the rest of the blue copper sites. Hence, the geometry of the active center is trigonal planar in laccases (NNS acting as equatorial donor atoms, Fig 2D), trigonal bipyramidal in azurins (with S and O as weak axial donor atoms, Fig 2B), distorted tetrahedral in most BCPs (NNS equatorial atoms and another S atom as a weak axial ligand, Fig. 2A) and tetrahedral in stellacyanin (being NNSO the donor atoms, Fig. 2C).

Electronic structure

In its oxidized state, blue copper centers present an intense ligand-to-metal charge transfer (LMCT) absorption band at 590-600 nm, responsible for their acute color as well as for an anomalously small parallel ^{63,65}Cu hyperfine coupling in their EPR spectra [6,29,33].

The high degree of covalency of the copper-SγCys interaction is crucial to determine the electronic structure of these centers and, as a consequence, their singular spectroscopic features. In fact, the strong overlap between the Cu(II)($3d_{x2-y2}$) and the Sγ($3p$) orbitals is responsible not only for the BCP spectroscopic singularities but also, to a large extent, for their kinetic and thermodynamic (redox potentials) properties [34] (see below). Two sets of blue copper sites have been defined according to this interaction [35]. The first group is called *classic* blue copper sites. Azurin and plastocyanin are good examples of them. These sites present a π interaction between the

mentioned orbitals of the copper ion and the sulfur atom. As a result, the observed CT band is completely dominated by this π pure interaction. *Classic* blue copper sites present a unique band at *ca.* 600 nm. EPR spectra of *classic* BCPs are typically axial. The second group is formed by the *perturbed* blue sites, which present a band at 450 nm ($\varepsilon_{450}/\varepsilon_{600} \geq 0.5$) in the UV-visible absorption spectra and tetragonal distortion in EPR. The band at 450 nm arises from a σ interaction between the Cu(II)($3d_{x2-y2}$) and the Sγ($3p$) orbitals, which predominates to the π interaction, according to geometrical factors of the copper site in the different BCPs. Rusticyanin and pseudoazurin present *perturbed* blue sites.

The limit of this σ interaction is found in *green* nitrite reductases, where the tetragonal distortion is so acute that the highest energy visible band (*i.e.*, the band at 450 nm) is the most intense. Solomon and coworkers have studied this issue in depth [29,34,36]. They have related this interaction with the architecture of blue copper sites. Concretely, they have related the Cu-S interaction with the ϕ dihedral angle that the planes $CuN_{His}N_{His}$ y $CuS_{Cys}S_{Met}$ form (Figure 3). When this ϕ angle decreases, the σ interaction increases (*perturbed* and, in the last term, *green* sites) and *viceversa* (*classic* blue copper sites).

Cupredoxin family

Blue copper sites are found in all domains of living organisms [10]. The presence of BCPs, also called cupredoxins (small and generally soluble proteins), is more restrictive. In fact, while BCPs are extensively located in bacteria and archaea, cupredoxins only exist in the plant chloroplasts in eukaryota.

Copper(I) and copper(II) oxidation states are easily interchangeable in these proteins (see below), thus allowing an efficient electron transport. To make this process possible a rigid three dimensional structure maintained upon electron transfer is required [37]. This is achieved thanks to the existence of a robust β-barrel conformation together with an extended hydrogen bond network that is common to all cupredoxins [38].

Table 1 summarizes the most distinctive features of some relevant cupredoxins. A picture of the basic global architecture of BCPs together with a brief description of the function of each protein follows.

Plastocyanin

Plastocyanins (Pc) [39-41], being the BCPs with the lowest molecular weight (97-99 amino acids, depending on the species), present the minimal tertiary structure common to all BCPs (Figure 4A). It consists in 8 β-strands aligned in a parallel or anti-parallel way to form two β-sheets that, in turn, shape a barrel structure. This topology is known as Greek key β-barrel. In the so-called *northern* side of the molecule is sited the copper ion. Three of the metal ligands (the cysteine, a histidine -HisC[1]- and the methionine) are located in the same loop. The cysteine and the methionine are, in fact, at the ends of strands 7 and 8, respectively, while HisC is in the middle of the loop. These three ligands are close in the primary structure in all BCPs (see ligand numeration in Table 1). The sequence CXXHXXXXM is kept for all plastocyanins. The other histidine (HisN[1]) is also located in a loop, at *ca.* 40-50 amino acids before the cysteine ligand. Therefore, the two histidines are located in flexible loops of the protein, while the sulfur donor ligands are localized at the end of rigid β-strands. This structure as well as the arrangement of the amino acids are common to all BCPs [42,43]. It is also remarkable that HisC is, in all BCPs, the most exposed ligand and, for this reason, the electrons flow through this histidine when the electron transfer reaction takes place [34,44].

Plastocyanin (Pc) is a component of the photosynthetic system [40,41]. It shuttles electrons from the cyt b_6f to the photosystem I (PSI). Biological electron transfer usually takes place when proteins face their crucial residues in such a way that reversible and fast complexes are formed. This type of adducts are called *transient* complexes. They are maintained just the time for electron transfer to befall. Two regions of different nature in Pc surface have been described. The so-called hydrophobic patch consists of 7-10 non-polar residues surrounding the most exposed histidine ligand of the copper ion (HisC). This patch is present in all BCPs [45]. A second domain, adjacent to Tyr83 (Pc poplar numeration[2]), is rich in acidic amino acids (residues 42, 43 and 61 are aspartate, while residues 42, 59, and 60 are glutamate). This negatively charged area seems to be exclusive of plastocyanins and, in fact, they have not been found in other BCPs. Pc receives an electron from cyt *f*, the specific intermembrane domain of the cyt b_6f complex that interacts with plastocyanin. Cyt *f*

[1] From now on, we will call this histidine as HisC, proximal in the primary sequence to the C-terminal extreme. The other histidine ligand will be denominated as HisN (proximal to the N-terminal end in the sequence of amino acids).

[2]In poplar plastocyanin the ligands HisN, Cys, HisC, and Met correspond to His37, Cys84, His87 and Met92.

heme group is located at the lumen side. This cytochrome presents a region rich in lysine residues (58, 65, 66, 165, 185 and 187, cyt *f* poplar numeration). The three dimensional structure of the complex between plastocyanin and cyt *f* has been solved by paramagnetic Nuclear Magnetic Resonance (NMR) both for poplar [46] and *Spinacia oleracea* [39]. Figure 5A displays the location of these residues in the surfaces of interaction between both proteins. Plastocyanin acidic residues are faced against positively charged cyt *f* residues (Figure 5B). Nevertheless, the largest surface area in contact with both proteins concerns to their respective hydrophobic patches.

Hydrophobic interactions are essential in electron transfer. Both research with mutated proteins in this patch and theoretical studies have shown that electron transfer paths concern residues belonging to these regions [39]. His87 in Pc and Tyr1 in cyt *f* are involved in most of the simulations performed on this system. In one of the plausible pathways described for poplar Pc-cyt *f* system the electron would flow from the heme group to Phe4 and then to Tyr1 (both belonging to cyt *f*). Finally, the electron would get the copper ion via Pc His87 [39] (Figure 5C). However, the electronic path depends on the Pc species: it is not even clear the specific amino acids implicated on it, although they always belong to the hydrophobic patch.

Plastocyanin transfers electrons to photosystem I (PSI). The PSI subunits PsiF and PsiN are involved in this interaction. While PsiF is a transmembrane protein, PsiN, present only in green algae and plants, is entirely located in the lumen side, where Pc–PSI interaction takes place. It has been proposed a mechanism for the docking between Pc and PSI [47]. According to it, the interaction occurs in two steps. In the first step, the acidic Pc surface interacts with the PsiF basic residues. When the transient complex is formed the hydrophobic contacts are essential and the Tyr83 non-polar surroundings are again crucial in electron transfer. Additionally, transgenic *Arabidopsis* plants lacking the PsiN subunit significantly decrease the electron transfer from Pc, suggesting an important role of this subunit in its docking with Pc [48].

Azurin

Azurin (Az, Figure 4B) is located in different denitrifying bacteria such as *Pseudomonas* or *Alcaligenes* [38,49]. Its function is closely related to denitrifying processes. As all BCPs, azurins have the classical β-barrel Greek key tridimensional

structure. Compared to plastocyanin, Az harbors an additional α-helix: whereas the number of amino acids in plastocyanins does not reach the hundred, azurins from different species contain between 120 and 130 amino acids. The aromatic amine dehydrogenase (AADH) is an Az electron acceptor. The crystal structure of the complex between these two proteins from *Alcaligenes faecalis* has been solved ([50]). Figure 6 shows this structure. The interface between both proteins covers *ca*. 550 $Å^2$. Twelve out of the 17 azurin residues that are in contact with AADH are hydrophobic (see Fig. 6B), while 75% of the residues of the AADH interface are hydrophobic. There exists an interprotein hydrogen bond between AADH Pro106 carbonyl oxygen and Az Ser12Oγ.

Tryptophan tryptophylquinone (TTQ) is the redox AADH cofactor. The electron pathway from copper azurin to TTQ has been analyzed by molecular modeling [50]. The best pathway discovered in that study is shown in Figure 6C. The electron flows from the TTQ cofactor to Trp160 (AADH), afterwards it jumps to Phe153 (AADH), then to the exposed HisC (Az) and finally reaches the copper ion.

Azurin is probably the most studied soluble redox protein, being used as the paradigmatic example to experience and confirm long electron transfer processes in biological systems, i.e., the Marcus theory [51,52] (see below). In this sense, Gray's and Pecht's works [53-57] in the 70s and 80s are elegant and instructive studies on how to design experimental devices (modified azurins with attached electron acceptor/donor complexes) to confirm or refuse theoretical hypotheses. Since then, azurin continues to be the best small protein to check or postulate a multitude of premises related to BCPs, in particular, and electron transfer proteins, in general. Mutated azurins involving the metal loop have been also extensively used by several groups [58] to demonstrate the role of each individual amino acid (either a ligand of the metal or not) in modulating the stability of the center [59] or the relative stability of the redox states of the copper ion [38,60,61] (i.e. the redox potentials). Likewise, Az properties have been modulated inserting a complete binding loop of another BCP in the own scaffold of azurin [61,62] (see below). Azurin has also been a model to postulate the role of the metal ion in the unfolding processes of metalloproteins as well as the stabilization of the whole protein [58,63-69]. Finally, and in some degree even surprisingly, peptides derived from the azurin primary sequence have been found useful as anticancerous agents (see last section).

Rusticyanin

Acidithiobacillus ferrooxidans is a Gram negative bacterium that lives in extremely acidic media (pH lower than 2.5) [70]. It obtains its energy from the oxidation of iron(II) ions by a dioxygen molecule [71]. The BCP rusticyanin (Rc) is the most abundant soluble protein of this organism. Rc participates in the electron transfer chain of *A. ferrooxidans*: it accepts electrons from the high molecular weight cytochrome *c* Cyc2 (iron:rusticyanin reductase) and it donates them to either the periplasmic cytochrome c_4-type Cyc1 (downhill electron transfer pathway, finishing in the O_2 reduction) or to the cytochrome CycA1 (uphill electron transfer pathway, that finishes in the NAD^+ reduction) [72]. Rc is the BCP with the highest redox potential (680 mV at physiological pH; 620 mV at neutral pH, see Table 1) and so it has been used as a good candidate for determining the factors that rules the redox potentials in BCPs (see below) [73]. Regarding other BCPs, Rc extends its N-terminal extreme by 35 additional amino acids [74] (Figure 4C). This feature has been described as a factor that protects the hydrophobic patch of the protein contributing both to its high stability at low pH values (Rc is stable at pH values lower than 2) and to its elevated redox potential. Moreover, the metal is surrounded by a large number of hydrophobic residues and this has been shown as a decisive factor of the high redox potential of this BCP [75,76] (see below). None X-ray structure of Rc complex with any of their partners have been solved. However, the docking between Rc and cyt c_4 has been studied by means of molecular modeling [77]. The existence of two intermolecular hydrogen bonds between rusticyanin and cyt c_4 stabilizes the complex. In fact, His143Nε (Rc) is hydrogen bonded to both carboxylic oxygen atoms of Asp15 (cyt c_4). Likewise, Thr 146Oγ forms a hydrogen bond with Ala8CO. The redox potential of Rc is reduced by 120 mV upon formation of the complex with its redox partner. The formation of the first hydrogen bond would then stabilize copper(II) form. The electron pathway through both proteins has also been calculated [78] and it seems to follow the route Cu—His143(Rc)—Asp15(cyt c_4)—hem group. Thus, the electron would flow just through the described hydrogen bond.

Amicyanin

Amicyanin (Am) is also an extremely well characterized BCP [79]. It is found in methylotrophic bacteria, being an indispensable protein in the conversion of methylamine into formaldehyde. Am accepts electrons from the enzyme methylamine dehydrogenase (MADH) and it donates them to a cytochrome c_{551} [80]. The crystal structure of the complex MADH-Am-cyt c_{551i} from *Paracoccus denitrificans* has been solved [81]. Numerous mutations have been carried out in Am metal binding loop [38,42,59,82]. By changing individual residues or a sequence of amino acids in the metal binding site Am has been converted into an azurin- or a plastocyainin-like active center. As in the complex between plastocyanin and cyt *f* [46] or between azurin and AADH (see above and Figures 5 and 6), MADH interacts with amicyanin through the hydrophobic patch [83], confirming again the crucial role of the hydrophobic core of cupredoxins both in the formation of the transient donor-acceptor complexes and in the electron transfer processes. Nevertheless, comparing Am-MADH and Az-AADH, the orientation of the BCP in relation to the dehydrogenase donor changes and, consequently, the number of residues in the interface of both proteins is modified as well, being lower in the former. Intermolecular hydrogen bonds are not present in the Am-MADH complex.

Other BCPs

Auracyanin (Au) is a BCP present in the *Chloroflexi* phylum of facultative aerobic phototrophic bacteria [84]. Different Au types have been described [84,85]. While auracyanins A, B and RC present *classic* blue copper sites, auracyanins C and D harbor *perturbed* sites. The function of the former auracyanins is believed to be related to electron transfer in both respiration and photosynthesis processes. Auracyanin C is believed to be involved in nitrite reduction. AuD, with a highly distorted blue site (the band at 450 nm present an absorbance even larger than that at 600 nm, consequently is a *green* site), have a very low redox potential (83 mV, see Table 1). As in stellacyanin, the copper axial ligand of AuD is also a glutamine [85]. Although it has been studied, it has not been found yet any relation between this two strikingly features of AuD.

Halocyanin is found in the haloalkaliphilic *Natronobacterium pharaonis* [86]. This aerobic archaea lives in media with high sodium chloride concentrations (*ca.* 3-4 M) and elevated pH values (higher than 8). Halocyanin is also characterized by its low redox potential (120 mV, see Table 1), although it presents a *classic* blue copper site

[87]. Pseudoazurin is, as Az and Am, a BCP located in denitrifying bacteria. Contrary to Az, its function has been demonstrated *in vivo* [88]: it donates electrons to nitrite reductase [89,90].

The glycoprotein stellacyanin (St), present in the tree *Rhus vernicifera,* deserves a special mention because of its singular axial glutamine coordination [30,31] (see Figure 2C). Uclacyanins [91] and plantacyanins [92] are BCPs found in *Arabidopsis thaliana*, although plantacyanin is also present in other different gender of plants. The crystal structure of spinach plantacyanin has been solved [93]. The functions of plantacyanins have been related to the plant defense responses [94], reproduction [92] as well as signaling molecules [95].

Factors modulating the redox potentials

BCPs are biomolecular devices for shuttling electrons. The driving force for such electron transfer is the difference of the redox potential of the implicated proteins. While the redox potential of the pair Cu(II)/Cu(I) in aqueous solution at pH 7.0 is 120 mV, the equivalent values for cupredoxins span from 85 mV (AuD) to 620 mV (Rc), i.e., a difference larger than 500 mV. Table 1 displays the redox potentials for most significant cupredoxins. It is certainly surprising such a large disparity in these theromidynamic parameters if we take into account that metal ion coordination is very similar for all BCPs (see Figure 2). The singular geometry of copper in BCPs is one deciding factor that modulates their redox potentials. Additionally, whatever factor that provides electron density to the metal ion stabilizes the oxidized Cu(II) form, and thus, decreases the redox potential. On the contrary, a hydrophobic environment destabilizes the most charged form of the metal ion (reduced form), increasing the redox potential [75,76].

Consequently, the redox potentials in cupredoxins strongly depend on three factors, namely: copper geometry, the donor atoms of the copper ion (inner coordination sphere) and modifications in the surroundings of the metal ion ligands (outer coordination sphere). There follows a detailed description of these three factors.

Coordination geometry: Entatic/rack-induced state

Evolution has designed active centers in BCPs with redox potentials higher than that of the pair copper(II)/copper(I) in aqueous solution (Table 1). Copper(II) type 2

complexes, i.e., those whose geometry is completely chosen by the metal preferences (see Figure 1A), usually are plane-square or octahedral with strong tetragonal distortion (Jahn-Teller effect). On the contrary, type 1 centers (Figure 2) present the following geometries: pseudo-tetrahedral (Pc or Rc, Fig. 2A), tetrahedral (stellacyanin, Fig. 2C), trigonal bipiryamidal distorted (azurins, Fig. 2B) and trigonal planar (laccases, Fig. 2D). Neither of these geometries are preferable for copper(II): copper(II) is found in a strained coordination, the so-called entatic or rack induced state [96].

The entatic/rack-induced state was postulated in parallel by Malmström [97] and Vallee [98] in the 1960s. The concept was applied not only to blue copper sites, but also to other metalloenzymes, such as zinc enzymes. The entatic/rack-induced state assumes that a rigid global folding present in a metalloprotein imposes a tense coordination to the metal ion. In turn, this rigidity is due to the extent of a network of hydrogen bonds indispensable for electron transfer. Copper ion is not then found in any of its preferential geometries. This tense state is more acute for the oxidized than for the reduced copper. Consequently, copper(II) is destabilized and the pair copper(II)/copper(I) redox potential is increased.

Although it has been debated in some extent [99,100], there exists a large number of experimental data that support validity of the entatic/rack-induced state [6,101]. We will comment here two of these evidences related to the redox potential of copper in both the folded (tense) and unfolded (relaxed) forms of a singular BCP, rusticyanin [102,103].

First, copper in BCPs is basically coordinated to two nitrogen and two sulfur atoms (see Figure 2). Copper(II) has a strong affinity by N-donor atoms; the existence of two imidazol rings in the coordination sphere of BCPs ensures the binding of the metal ion in this oxidation state to the protein. Copper(I) has a high affinity by sulfur atoms, so the existence of the cysteine and the methionine ligands would stabilize the reduced state and would increase the redox potential. Being this true, the two sulfur ligands by themselves cannot be the unique factor, neither the main one, for explaining the increase of the redox potential in relation to the copper(II)/copper(I) aqueous pair. In fact, rusticyanin [102] as well as azurin [104] bind copper in their unfolded forms. Concretely, copper is bound to a histidine (HisC) and to the same sulfur donor atoms as in the folded state. In other words, when the unfolding process takes place HisN, being located far away in the primary structure (see Table 1, ligand numbers), is detached from the metal ion, while the loop C138XXXXH143XXXXM148 (Rc sequence)

continues being attached to it. Having the copper in this unfolded form a larger ratio of sulfur atoms than in the folded form (2:1 is the ratio sulfur versus nitrogen atoms in the unfolded state, the ratio is 2:2 for the folded form), the redox potential continues being larger for the folded than for the unfolded form. Thus, not only the nature of the donor atoms, but the architecture of the active center (entatic for the folded form, relaxed for the unfolded form) has to be decisive.

Secondly, to further discern the factors that determine the redox potential in BCPs, a thermodynamic cycle was described both for the folded and the unfolded proteins [103]. In such a cycle, depicted in the Scheme 1, the Gibbs free energy based on the reduction potential of rusticyanin, ΔG(1)(CuRc), is related to three contributions according to the following equation:

$$\Delta G(1)(CuRc) = -\Delta G(3)(Cu(II) + Rc) + \Delta G(2)(Cu) + \Delta G(4)(Cu(I) + Rc) \quad [1]$$

where ΔG(3)(Cu(II)+Rc) and ΔG(4)(Cu(I)+Rc) are the Gibbs free energies concerning the formation of the holoproteins starting from the apoBCP for the oxidized and reduced states, respectively; and ΔG(2)(Cu) corresponds to the Gibbs free energy associated to the redox reduction of the pair copper(II)/copper(I) ion in aqueous solution (see Scheme 1).

The ΔG values for reactions (1), (2) and (3) were experimentally determined both for the folded and unfolded proteins and then, ΔG values corresponding to reaction (4) were deduced in both forms. These values are given in the same Scheme 1. Subsequently, a comparison between the affinities of copper(II) and copper(I) for the folded protein was obtained, with resultant values of -11,4 and -20.6 kcal/mol. In other words, the protein in its native state stabilizes copper(I) by 9.2 kcal/mol, that accounts for the high redox potential of rusticyanin. Analogous calculations for the unfolded forms gave values for the equivalent processes of -9.4 and -16.3 kcal/mol, respectively. Therefore, the ligands only stabilize copper(I) versus copper(II) by 6.9 kcal/mol in the unfolded form. As stated by the rack/entatic mechanism, it follows that folding is essential in stabilizing copper(I) versus copper(II), i.e., in maintaining the high redox potential of rusticyanin.

It is important to remark that not only the tertiary structure of BCPs stabilizes copper binding but also the binding of copper ion stabilizes BCP tertiary structures. In

fact, several studies have shown that apoBCPs are less stable towards unfolding than holoBCPs [102,105]. In this last case, reduced BCPs are more stable than oxidized cupredoxins.

Inner coordination sphere

The most common donor atoms of the copper ion in BCPs are two sulfur and two nitrogen atoms (Figure 2A). The axial methionine is a crucial ligand in tuning the redox potentials of cupredoxins. Furthermore, typical Cu-SγMet distances in model complexes are substantially shorter (*ca.*2.3 Å) than those found in BCPs (around 2.9 Å) [106]. This long copper-axial ligand distance reduces the electron density that the sulfur provides to the metal ion and thus, copper(II) is destabilized in relation to copper(I). Consequently, this factor increases the redox potentials. Numerous studies with mutants in the axial ligand have been performed in several cupredoxins [107,108]. The replacement of the axial methionine by a ligand containing an oxygen donor atom, such as a glutamine, decreases the redox potential of Az by 121 mV [108], Am by 85 mV [109] and Rc by 148 mV [110]. On the contrary, replacement of the axial ligand by a non-coordinating amino acid, for instance Ala or Leu destabilizes copper(II) and thus, increases the redox potential by more than 100 mV, depending on the specific cupredoxin (Rc *ca.* 180 mV [111], Az *ca.* 100 mV [107]. It is important to consider that the highest redox potential of a blue copper site corresponds to human ceruloplasmin (*ca.* 1000 mV [112]), whose coordination is analogous to that of some laccases shown in Figure 2C.

Replacement of the equatorial cysteine ligand has been also reported [32]. Gray's laboratory has obtained the azurin mutant Cys112Asp; this protein loses the typical BCP spectroscopic features and thus, the center is no longer a T1 copper site. The resultant T2 center shows a redox potential as low as 180 mV (Az wt redox potential is 276 mV, see Table 1). Further axial methionine substitutions in this mutant partially reverse the spectroscopic and electron transfer behavior of the native copper center resulting in the so-called type zero centers (Figure 2E).

Equatorial histidines have also been replaced in several cupredoxins. His143Met Rc mutant (HisC) has been successfully obtained and its crystal structure solved [113]. Its redox potential has not been experimentally determined due to its high value, although it is calculated to be over 400 mV higher than that of Rcwt. Furthermore, Canters and coworkers have deeply studied His117 (HisC) azurin mutants [114,115].

Depletion of this histidine produces a hole where several small ligands can bind to the metal ion loosing (or not) the "blue" character of this mutated protein [115].

It is also significant that azurin has a fifth, weak, ligand: the carbonyl oxygen of a glycine (Gly45, Figure 2B). The contribution to the redox potential of this oxygen has been obtained by the mutation Phe114Asn [107]. Phe114 is close to Gly45. This mutation generates a hydrogen bond between the carbonyl oxygen and Asn114, disrupting the interaction between the copper ion and the carbonyl oxygen. The mutation increases the redox potential of azurin from 276 to 398 mV. Consequently, the effect of removing the electron density donated by this oxygen to the copper ion is, as expected, an increase in the azurin reduction potential.

Outer coordination sphere

A network of hydrogen bonds close to the copper finely tunes the redox potential of BCPs. This network is also essential for the electron transfer (see below). In all BCPs, the sulfur atom of the cysteine ligand forms one or two hydrogen bonds with backbone amides from adjacent residues. In Rc, Ser86 and Ile140 amide protons generate hydrogen bonds with the Cys-Sγ atom (Rc ligands are listed in Table 1). Figure 7A displays the strands where the ligands His85 (HisN) and Cys138 are located. In turn, Ser86Oγ atom forms hydrogen bonds with Gln139. The equivalent position to Ser86 is a highly conserved Asn in the rest of BCPs. The mutation Ser86Asn reduces the Rc redox potential by 77 mV [116]. This decrease is due to the loss of the hydrogen bond in the Ser86Asn mutant. Conversely, mutation of the equivalent Asn by a Ser in azurin increases its redox potential by 130 mV [107]. These inter-loop interactions provide rigidity to the metal site modulating the redox potential and also facilitating electron transfer (see below).

Likewise, the loop HisC-Met contains from 5 to 7 hydrogen bonds, depending on the specific BCP, that modulate the interaction of these two ligands with the metal ion. Again, taking as an example, rusticyanin, 5 H-bonds are found in this loop (Figure 7B). This loop is also crucial in electron transfer since HisC (His143 in Rc) is directly implicated in long-range biological electron transfer.

Finally, it should also be considered the effect of the polar/non-polar nature of the metal ion environment. For instance, the copper ion of rusticyanin (the cupredoxin with the highest redox potential) is surrounded in a large extent by hydrophobic residues

that stabilizes copper(I). By means of paramagnetic NMR performed on the Co(II)Rc derivative [75], it has been observed that up to five phenylalanines (Phe54, 51, 76, 83 and 111) and one isoleucine (Ile140, Figure 7C) are close enough to the metal ion to experience large dipolar (through space) shifts. This indicates that these amino acids are strongly affected by the nature of the metal ion, what is reflected in their chemical shifts. Likewise, the metal ion deeply experiences the effect of the hydrophobic aminoacids as well. This feature has been described as one of the factors that increase the redox potential of Rc in relation to others BCPs [75,76].

Electron transfer rates

According to Marcus theory [51], the electron transfer rate, k_{ET} (equation 2), depends on three critical factors, namely: the Gibbs free energy change upon electron transfer, ΔG^0; the electronic coupling factor between the reactants, H_{AB}; and the reorganization energy, λ.

$$k_{ET} = \left[4\pi^2 H_{AB}^2/h(4\pi\lambda RT)^{1/2}\right] exp[-(\Delta G^0 + \lambda)^2/4\lambda RT] \qquad [2]$$

The driving force ΔG^0, depends on the redox potentials of both participating proteins and can change when the transient complex is formed. For instance, when Rc interacts with its physiological partner, its redox potential diminishes by *ca.* 80 mV [117]. This decrease is necessary to close the energy gap between the donor and the acceptor in such a way that the electron transfer can take place. The electronic coupling, H_{AB}, depends on the distance between the active redox center and the nature of the medium, being optimum when the transfer is carried out through covalent bonds [118].

The reorganization energy (λ) deserves a special mention. This parameter can be described as the energetic cost entailed by the conformational change associated with the capture or the release of an electron by the protein. A low reorganization energy (λ) is required for the electron transfer over long distances (10-30 Å), those typically found between the electron donor and acceptor in biological systems. Therefore, type 2 copper complexes usually showλ values larger than 2 eV [119], what implies a high energy cost for the interconversion between both oxidation states. Type 2 complexes are inefficient for transferring electrons in natural processes. On the contrary, blue copper

centers present low λ values (0.6-0.8 eV) [120], allowing them to change their redox states very fast, for instance, with the high degree of effectiveness necessary for electron transfer to take place in nature. Hence, this feature arises from the high degree of covalency which is present between the Cu ion and the SγCys thiolate atom [34] (see above). Lastly, this is a consequence of the forced coordination of the copper ion by the protein scaffold. The entatic/rack induced state is necessary for electron transfer to take place. The hydrogen bond network previously commented is the key feature for maintaining the indispensable rigidity of the copper active sites for shuttling the electrons.

As it has been mentioned before, azurin has been used as the paradigmatic model to study electron transfer reactions in biological systems. Mutations in the outer coordination sphere have provided detailed information on the role of each specific interaction in the electron transfer. Up to this point, the role of the hydrogen bonds is particularly remarkable. For instance, studies with azurin mutants in positions Asn47, Phe114 and Met121 have been performed [121]. All mutated proteins keep the blue character. Ligands in Az are $G_{45}H_{46}C_{112}H_{117}M_{121}$ (Table 1, ligands) thus, Asn47 is the following residue to HisN in Az (i.e., equivalent to Ser86 in Rc, see Figure 7A), Phe114 is sited two residues after the cysteine ligand in the aminoacid sequence (the equivalent position to Ile140 in Rc, see Figure 7A) and Met121 is the methionine axial ligand. Strictly speaking, the three amino acids belong to the inner (Met121) or to the closest outer (Asn47 and Phe114) coordination spheres. The intramolecular ET rates for all studied mutants were higher than that of Az wild type. In fact, the ET rates ranged from 78 $\pm$12 s^{-1} for the triple mutant Asn47/Phe114Asn/Met121Leu to 387 $\pm$ 59 s^{-1} for the double mutant Asn47Ser/Phe114Asn mutant (Az wt ET rate value was 44$\pm$ 7 s^{-1}). Furthermore, the calculated reorganization energy was also significantly lower than that of Az in all cases. In particular, Az wild type presented a λ value of 1.21 eV, while the lower λ value for the studied mutants corresponded to the triple aforementioned mutant (0.71 eV). On the contrary, the highest value for the lambda of the mutants (that of the double mutant Phe114Asn/Met121Leu) presented a value of 0.94 eV. The authors associated these differences in λ and the ET rates to changes in the hydrogen bonds and consequently, in the degree of rigidity of the outer coordination sphere in the diverse mutants.

Similar studies with mutants in amicyanin have also been carried out [122].Am Met98Gln mutant (Met98 is the axial methionine in *Paracoccus denitrificans* amicyanin) reduces the electron transfer rate between MADH and Am by 45-fold in relation to amicyanin wild type. Concomitantly, the reorganization energy is increased by 0.4 eV. The authors associated this increment in the reorganization energy with a displacement of the copper ion from the NNS plane of the equatorial ligands (0.20 Å in Am wt, 0.42 Å in Am Met98Gln). In conclusion, this mutationin the inner coordination sphere favors one redox state (the oxidized) versus the other (the reduced). This implies larger structural changes when the electron is accepted or donated with the subsequent considerable energetic cost (λ increment).

A compromise: rigidity of the holocupredoxin versus flexibility of the apoBCP

Rigidity of the active center is a mandatory feature required for the blue copper sites to efficiently perform their functions. The entatic/rack picture explains both the high redox potentials and the low reorganization energies of BCPs. The solved X-ray structures of several apo-cupredoxins [123-127] revealed that holo and apoBCP tertiary structures were practically identical. This included the amino acids located in the copper active site: this cavity continued being rigid even in the absence of the metal ion. It was assumed as a clear evidence of the existence of a preformed hole in the apoprotein cavity, inflexible even before copper uptake. Evolution had designed these sites to "force" copper to bind apo-cupredoxins as dictated by their scaffold. These data strongly stood for the entatic/rack hypothesis.

This last idea presented a conceptual dilemma that is difficult to resolve when copper uptake *in vivo* is accounted for. Before setting out the problem, a description of how copper ion is loaded by metalloproteins has to be briefly defined. Copper centers *in vivo* are formed through the medium of metallochaperones [128-130].In fact, no free copper is available in the cell. Thus, the possibility that an isolated copper ion can diffuse in the cell until it is captured by the corresponding apoprotein has to be discarded [129]. It is essential to contemplate that excess copper is toxic due to the generation of the reactive oxidative species (ROS) via the Fenton reaction: the reducing ambient inside the cell forces copper to remain in its oxidation state +1.

In eukaryotes Atx1 metallochaperones delivers copper(I) from the plasma to other cytosolic metallochaperones (such as P-type ATPases proteins, among others

[128]). Regarding green algae, two different classes of P-type ATPases have been found in chloroplasts (namely; P-type 1 ATPases 1, PPA1, and 2, PAA2) [131]. Functional studies with mutated PAA1 and PAA2 in *Arabidopsis thaliana* have come to the conclusion that the former metallochaperon imports copper(I) into the stroma, while the latter directs this ion into the thylakoid lumen, where plastocyanin uptakes copper(I).

Likewise, in cyanobacteria lacking specific copper(I) ATPases PacS and CtaA, photosynthesis is spoilt by deactivation of Pc and cytochrome oxidase [132]. Accordingly, these ATPases have been considered decisive in copper uptake by Pc. In *Pseudomonas aeruginosa*, the lack of CopA1 and CopA2 (Cu(I)ATPases) induces the transcription of azurin as a consequence of the increase in the ROS species. Although non specific metallochaperon for azurin has been described up to date, this type of experiments strongly suggests the participation of these ATPases as metallochaperones for Az. In the Gram-negative bacterium *Thermus thermophilus*, a direct transfer from the periplasmic metallochaperon PCu_AC to its ba_3 oxidase generating the CuA holoprotein (Figure 1C) has been demonstrated *in vitro* [133]. Furthermore, the loading of copper has to be a well-directed process taking into account the high energetic cost that protein synthesis implies for the cell: wrong metallations have to be precluded [134]. Thereby, although up to the knowledge of the authors there is still not a primary evidence of a metallochaperone involving the cession of copper to any specific BCP *in vivo*, a large multitude of evidences indicates that this is the most reasonable process.

Since no free copper is present in the cell, the process consisting in the releasing of the copper by the metallochaperone and the instantaneous loading of the metal ion by the apo-cupredoxins is only possible if ligands belonging to both proteins are simultaneously bound to the copper ion. This has been observed in the formation of the holo-CuA *T. thermophilus* ba_3 oxidase *in vitro*, as previously commented [133]. For such intermediates to occur, the active centers of apoBCPs should be flexible enough to be opened to interact with the metallochaperone and to construct the blue copper site. Consequently, a strong contradiction arises: if the apoprotein active site were rigid as early X-ray studies seemed to reveal [123-127], then, how can copper be loaded by the apoprotein *in vivo*? In other words, how can the active holoprotein efficiently be formed *in vivo*? As commented heretofore, it seems that there was a conflict between the supposed rigidity of the preformed site of the apoform, ready to uptake copper, and the necessary metal site flexibility of the apoprotein needed *in vivo* to load the copper ion from the metallochaperones.

Such apparent disagreement was reconciled when dynamics heteronuclear, ^{1}H-^{15}N, NMR studies on apoazurin *in solution* were carried out [135].Relaxation measurements of ^{1}H-^{15}N NOE, ^{15}N transversal relaxation rates, R_2, and ^{1}H and ^{15}N Chemical Shift Perturbations, CSP, were performed. Figure 8 display a map of the Az tertiary structure showing the most relevant results of this research. As observed, not only the metal ligands but also the amino acids close to the active site display mobilities in the microsecond to second timescales. Thus, apo forms of BCPs are flexible and close enough to the metal site. Consequently, they can interact with metallochaperones to efficiently load copper *in vivo*.

Recently, molecular dynamics studies performed on Az and St have revealed that HisC in the apoprotein is highly flexible, being the Nδ1 imidazol atom exposed to the solvent most of the time [101]. According to these simulations, authors suggest that such atom is implicated in capturing copper and the formation of the blue copper site by a rotation of HisC.

The discrepancies of these new data with previous results, obtained from X-ray studies, could arise from two different causes. First, all except one of the apo forms in the solid state studies [123-126] were obtained by, initially, crystallizing the holoprotein and, afterwards, by sequestering the metal with the corresponding chelating agent from the apo form. Second, crystal package effects can also have decisive consequences in the dynamics of the active site. Anyhow, *solution* NMR data clearly demonstrates the flexibility of the active site surroundings in the apoBCPs. This fact can explain the ability of apoproteins to form simultaneous complexes with metallochaperones, being this necessary for copper uptake *in vivo*.

This last idea was referred to the apo form, so no refutation of the entatic/rack-induced mechanism was performed in the most recent study. It is important to consider that the entatic/rack-induced mechanism is always related to the holoprotein. In other words, although apo forms are specifically designed to conform a rigid site when the metal ion binds, they have enough flexibility to interact with their metal donors (metallochaperones).This is the key for reconciling, on one hand, the exigency of rigid holoproteins to carry out their own biochemical processes (electron transfer) and, on the other hand, the necessity of flexible apo-cupredoxins to efficiently load copper ions from the metallochaperones.

BCPs as therapeutic agents

Azurin in cancer research

Therapy against cancer is one of the major issues in Chemistry research in the last decades. All type of drugs has been synthesized and experienced *in cellulo* and *in vivo* [136-139]. Most compounds used as anticancer agents are nowadays not selective towards tumor cells and interact, to a large extent, with very different proteins and nucleic acids of healthy cells. This causes the well-known side effects in patients. It is crucial to find new anti-cancer species with two features: first, high selectivity towards the tumor cells; and second, as a consequence, a drastic reduction of their toxicity.

In this sense, proteins arising from bacteria and virus seem to be a new promising line of research [140,141]. Concretely, azurin has anticancer activity against MCF-7 breast cell lines [142,143]. EphB2 tyrosine kinase, overexpressed in several lines of cancer, is associated to the abnormal grown of tumor cells as well as with the formation and proliferation of blood vessels in tumors (angiogenesis). Plastocyanin, azurin and rusticyanin have structural similarities to ephrinB2 [144], the activating ligand of the receptor EphB2 tyrosine kinase. Likewise, alignment of Pc, Az, and Rc crystal structures with that of this last protein resulted in root mean squared deviation (rmsd) values of 1.8, 3.4 and 3.1 Å, respectively. In particular, the loop encompassing the amino acids 88 to 113 in Az shows a high similarity with the domain (amino acids 84-112) of ephinB2 (Figure 9). While commercial drugs for inhibiting EphB2 are not selective (toxicity effects), azurin competes with ephirinB2 for the same binding domain in EphB2. As a consequence, azurin action is highly specific.

Another relevant region of azurin is that encompassing the amino acids 50-77 (Figure 9). A peptide derived from azurin sequence, p18 (amino acids 50-67) contains an α-helix and several hydrophobic residues. This p18 peptide behaves as a cell-penetrating peptide (CPP). Nevertheless, it does not show any cytotoxic effect in the cell [145]. On the contrary, an extent of this peptide, p28 (amino acids 50-77) exhibits a strong cytotoxicity against MCF-7 cells and, most importantly, it is selective in relation to healthy kidney or liver cells [146]. P28 interacts with the p53 binding domain hampering its degradation [147]. This gene acts as a tumor suppressor producing apoptosis and cell cycle arrest, and consequently, its stabilization by the peptide p28 produces the mentioned effects on the cancer cells. The action of p28 has been undergone in clinical trials (phase I studies). Fifteen patients with different advanced tumors were treated with p28. Two of them experienced complete regression of the

cancer and other two partial regression [148]. No patients exhibited any secondary significant effects. Moreover, p28 has been shown to exhibit antiangiogenic behavior [149].

Not only azurin but also rusticyanin present citotoxicity effects. Both cause cell cycle arrest and apoptosis in J774 and human cancer cells [150]. Nevertheless, it seems that Rc lacks of the structural features of azurin in relation to cell penetrating properties [151].

Cupredoxins and viral infectious diseases

The effect of azurin, pseudoazurin, plastocyanin and rusticyanin on the virus cycle of *Plasmodium faciparum*, responsible for malaria infection has been studied and even patented [152]. As demonstrated by heteronuclear ^{1}H-^{15}N NMR [153], rusticyanin binds to the *Plasmodium* merozoite surface protein-1 (MSP1), in charge of the initial binding of the parasite to the host cell. Holo-rusticyanin binds $MSP1_{19}$ (the MSP1 19-kDa C-terminal fragment) by its northern face, i.e., close to the copper ion. Moreover, the binding depends on the oxidation state of the copper ion: reduced Rc binds one order of magnitude tighter than copper(II)Rc. Azurin and plastocyanin does not exhibit such a high interaction with $MSP1_{19}$.

Finally, it is interesting to highlight that the interaction between azurin and the envelope glycoprotein of the human immunodeficiency virus type-1 (HIV-1) has been reported [154]. Nevertheless, no inhibitor potential of azurin towards this virus has been demonstrated so far.

Acknowledgements

This work has been financially supported by the Spanish *Ministerio de Economía y Competitividad*, FEDER (Project SAF2011-26611) and the *Fundación Séneca de la Región de Murcia* (Project 15354/PI/10). L.A.A. also acknowledges the *Spanish Ministerio de Economía y Competitividad*, Programme *Torres Quevedo*, for a grant (PTQ-11-04960).

Tables

Table 1. Relevant data of some representative BCPs, ordered by its redox potential.

Protein	MW[a] (kDa)	Origin	Kingdom	Redox partners	Function	Ligands	Coordination geometry[b]	pI[c]	Redox potential (mV)
Auracyanin D	12.8	*Chloroflexus aurantiacus*	Bacteria	*Molibdopterin oxidoreductase*[e]	Respiration, photosynthesis, nitrite reduction[f]	$H_{76}C_{114}H_{119}Q_{121}$	Tetrahedral (C)	4.0	83
Halocyanin	15.5	*Natronobacterium pharaonis*	Halo-archaea	Menaquinole/ halocyanin oxidase	Quinole oxidation	$H_{86}C_{124}H_{127}M_{132}$	Distorted tetrahedral (A)	4.5	120
Stellacyanin	20.0	*Rhus vernicifera*	Plant	Unknown	Unknown	$H_{46}C_{87}H_{92}Q_{97}$	Tetrahedral (C)	9.9	180
Pseudoazurin	13.4	*Achromobacter cycloclastes*	Bacteria	--/nitrite reductase	Denitrification	$H_{40}C_{78}H_{81}M_{86}$	Distorted tetrahedral (A)		260
Amycianin	13.8	*Thyobacillus versutu*	Bacteria	cytochrome c_{551}/ methylamine dehydrogenase	Methylamine oxidation	$H_{80}C_{119}H_{122}M_{125}$	Distorted tetrahedral (A)	4.7	261
Azurin	14.0	*Alcaligenes denitrificans*	Bacteria	cytochrome c_{551}/ nitrite reductase	Denitrification	$G_{45}H_{46}C_{112}H_{117}M_{121}$	Trigonal bipyramid (B)	5.4	276
Umecyanin	14.6	*Armoracia laphtatifolia*	Plant	Unknown	Unknown	$H_{44}C_{85}H_{90}M_{95}$	Distorted tetrahedral (A)	5.9	283
Mavicyanin	18.0	*Cucurbita pepo medullosa*	Plant	Unknown	Unknown	$H_{45}C_{86}H_{91}Q_{96}$	Tetrahedral (C)	8.9	285
Plantacyanin	10.1	*Cucumis sativus*	Plant	Unknown	Defense responses /Respiration/ signaling molecules	$H_{34}C_{74}H_{79}M_{84}$	Distorted tetrahedral (A)	10.5	317
Plastocyanin	10.5	*Populus nigra*	Plants, algae	cyt b_6f / PSI	Photosynthesis	$H_{37}C_{84}H_{87}M_{92}$	Distorted tetrahedral (A)	4.2	370
Rusticyanin	16.5	*Acidithiobacillus ferrooxidans*	bacteria	cyt *c* Cyc2 / c_4-type Cyc1	Aerobic Fe(III) oxidation	$H_{85}C_{138}H_{143}M_{148}$	Distorted tetrahedral (A)	9.1	620

[a] Molecular weight. [b] The letters between parentheses (A, B, and C) correspond to the ligands and the geometry displayed in Figure 2. [c] Isoelectric point. [d] Electrode potential values are referred to the normal hydrogen electrode scale. [e] Hypothesis, not confirmed [85]; [f] Respiration and photosynthesis are referred to Au A and B, nitrite reduction is referred to Au D, although it is not confirmed [85].

Caption to the Figures

Figure 1. Copper centers: A) Type 2, copper site of Cu/Zn superoxide dismutase from *Brucella abortus* (4L05 PDB code); B) Type 3, a tyrosinase from *Streptomyces castaneoglobisporus* (2ZMZ); C) Copper A, ba_3 cytochrome *c* oxidase from *Thermus thermophilus* (3S8F [155]); D) Copper B, cytochrome *c* oxidase (1V54 [156]); E) Copper Z, nitrous oxide reductase from *Paracoccus denitrificans* (1FWX [157]); F) Red copper, nitrosocyanin from *Nitrosomonas europaea* (1IBY [27]). See text for details.

Figure 2. Representative active centers of type 1 or Blue Copper Sites: A) Plastocyanin (4DP9 PDB code [158]), the most common site, with two equatorial histidines: one equatorial cysteine and one axial methionine as ligands; B) Azurin (4KOC), with an additional ligand oxygen carbonyl from a glycine in the *trans*-like position in relation to the axial methionine; C) Stellacyanin (1JER, [31]), with a glutamine as axial ligand, instead of the methionine; D) Laccase from *Trametes cinnabrina* (2XYB), without any axial ligands; E) Type zero protein (3FPY, [32], Cys and Met ligands from azurin (Fig. 2B) are substituted by an aspartate and a phenylalanine residue, respectively, resulting in a tetrahedral coordination. Upper panel: copper and amino acid ligands. Lower panel: copper and specific donor atoms (blue, nitrogen; yellow, sulfur; red, oxygen).

Figure 3. A) Scheme of the variation of the dihedral angle ϕ (the plane formed by the planes CuNN and CuSS) in *classic*, *perturbed* and *green* copper sites: the ϕ angle decreases in this series [36]. B) Interaction between the orbitals Cu(d_{x2-y2}) and SγCys(3*p*): when the ϕ dihedral angle is close to 90º (*classic* blue sites) a strong π interaction between both orbitals exists; on the contrary, when the ϕ angle is small (*green* sites) the interaction becomes σ type. C) UV-visible absorption spectra of *classic* (*c*), *perturbed* (*p*) and *green* (*g*) copper sites: the band at 450 nm (up arrow) increases (strong σ interaction) in this series, while the band at 600 nm (down arrow, strong π interaction) decreases.

Figure 4. Tertiary structures of some representative Blue Copper Proteins. A) Plastocyanin (4DP9 PDB code [158]); B) Azurin (4KOC); C) Rusticyanin (2CAK [113]). The Greek β-barrel, common to all BCPs, is drawn in blue color. The α-helixes, singular for each protein, are plotted in red. The location of the copper ion is shown in all cases as a blue sphere.

Figure 5. A) Overview of the solution structure of the complex between plastocyanin (white cartoon) and cyt *f* (brown cartoon) for poplar species (1TKW pdb code [159]). Pc negative aminoacids and cyt *f* positive residues mentioned in the text are colored as pink and yellow, respectively. Pc Tyr83 (green) and the cyt *f* heme group (red) are also displayed as a reference. The copper (blue) and the iron (orange) atoms are represented as spheres. B) Expansion of A, showing the contacts between negative and positive amino acids of both proteins. C) A closer view of the location of His87 (Pc), Tyr1 (cyt *f*) and Phe4 (cyt *f*) that could participate in the electron flow from the iron to the copper (see text [159]). Due to clarity reasons, the complex has been rotated in this last image.

Figure 6. A) Structure of the complex between azurin (white cartoon) and AADH (brown cartoon, only the subunit in contact with Az is shown) from *Alcaligenes faecalis* (2H47 PDB code [50]). Az hydrophobic residues are colored as pink. The intermolecular hydrogen bond between Ser12Oγ and Pro106CO (see text) is highlighted in green. The residues that participate in the electron transfer are shown in yellow. The copper atom is displayed as a blue sphere. B) Expansion of A, showing the hydrophobic residues and the indicated hydrogen bond. C) A closer view of the location of the proposed electron transfer path between copper Az and the AADH ligand TTQ (see text).

Figure 7. Three complementary views of rusticyanin active site (2CAK pdb code [113]). A) Plot of the aminoacids following the cysteine ligand (Gln139 and Ile140) and HisN (Ser86) ligands. Three H-bonds are displayed(plotted as discontinuous lines): two of them concerning to Cys138Sγ (with Ser86 and Ile140 amide protons) and the other formed between Ser86Oγ and the Gln139HN. B) Loop encompassing the aminoacids His143 (HisC) to Met148. Five hydrogen bonds are observed (plotted as discontinuous

lines). C) Hydrophobic residues that surround copper ion in Rc. The five phenylalanines are colored as green; Ile140 is plotted in red.

Figure 8. Backbone cartoon of azurin tertiary structure (4AZU PDB code [160]) showing the residues whose ^{1}H and ^{15}N amide nuclei parameters significantly change when apo and reduced forms are compared (copper ion, the blue sphere, it is displayed as a reference). A) Differences between the apo and the Cu(I) forms in Chemical Shift Perturbations, CSP: residues with CSP values lower than 0.2 (not perturbed) are shown in light grey; backbone nuclei with CSP values in the range from 0.2 to 0.5 (moderately perturbed) are colored in orange; CSP values higher than 0.5 (highly perturbed) are colored in red; residues with missing HN correlations are shown in yellow. B) Slow dynamics relaxation, ΔR_2, values: residues with ΔR_2 values lower than 2 s^{-1} (not perturbed) are displayed in light grey; residues with ΔR_2 values higher than 2 s^{-1} (highly perturbed) are displayed in orange; lost residues in the apoform are displayed in red. C) Sum of both effects, CSP and ΔR_2: NMR parameters of residues colored in light green do not change from the holo to the apo form; residues colored in orange are moderately perturbed; residues shown in red are highly perturbed. In the three panels proline residues are displayed in yellow. Most perturbed residues are located close to the metal site surroundings. Data adapted from reference [135].

Figure 9. Backbone cartoons of azurin (4AZU PDB code [160]) and ephirinB2 (1KGY [161]) tertiary structures (left panels).Right panels: upper, location of p18 (aa 50-67, orange) and P28 (aa 50-77) in Az; middle, location of p88-113 (violet); down, residues 88_114 in ephirinB2 (green). Two views of the peptides (rotated by 45º) are shown.

Figure 1

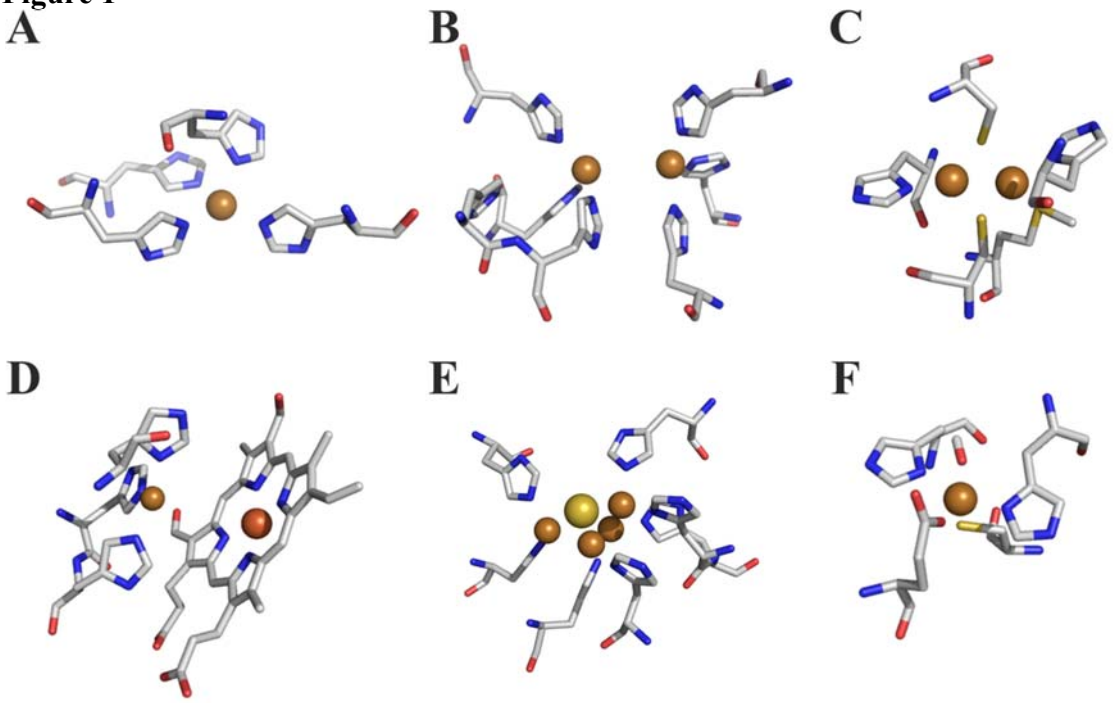

Figure 2

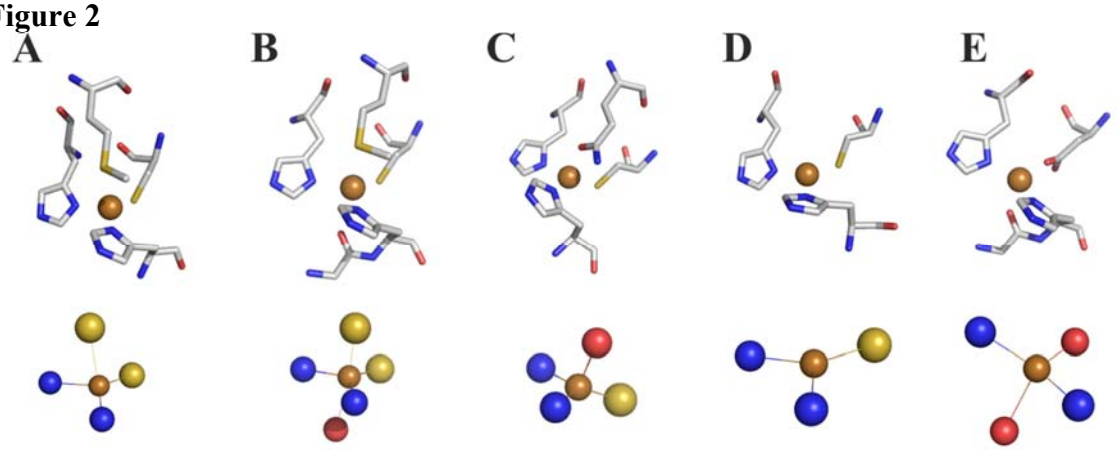

Figure 3

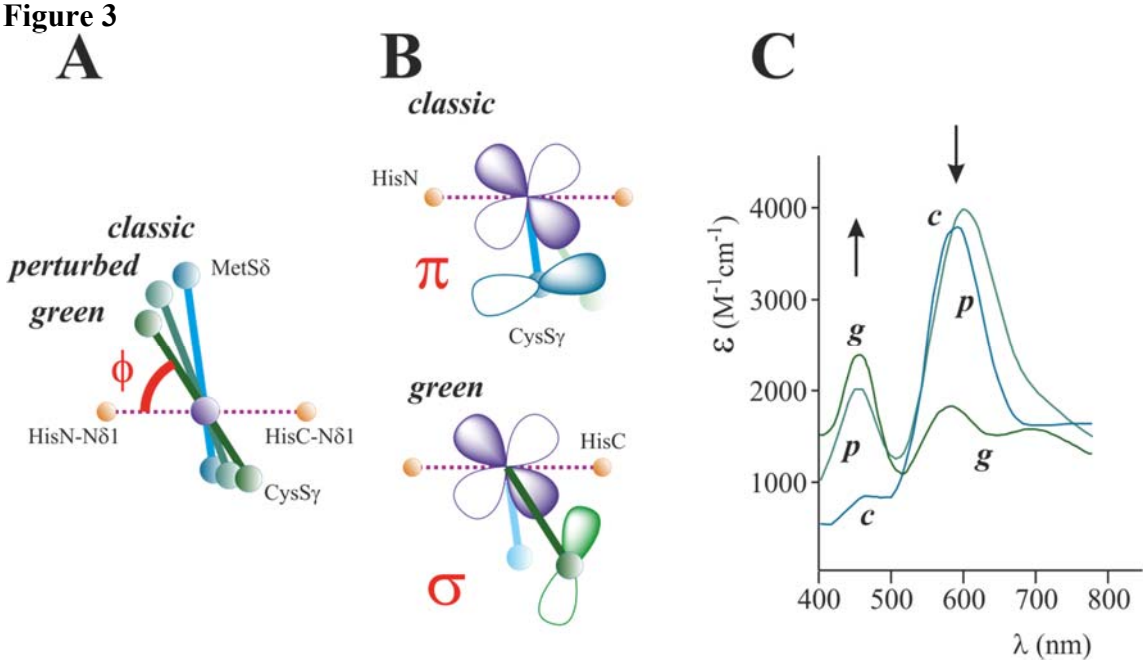
A
classic
perturbed
green
MetSδ
ϕ
HisN-Nδ1
HisC-Nδ1
CysSγ
B
classic
HisN
π
CysSγ
green
HisC
σ
C
ε (M-1cm-1)
4000
3000
2000
1000
c
p
g
p
g
c
400
500
600
700
800
λ (nm)

Figure 4

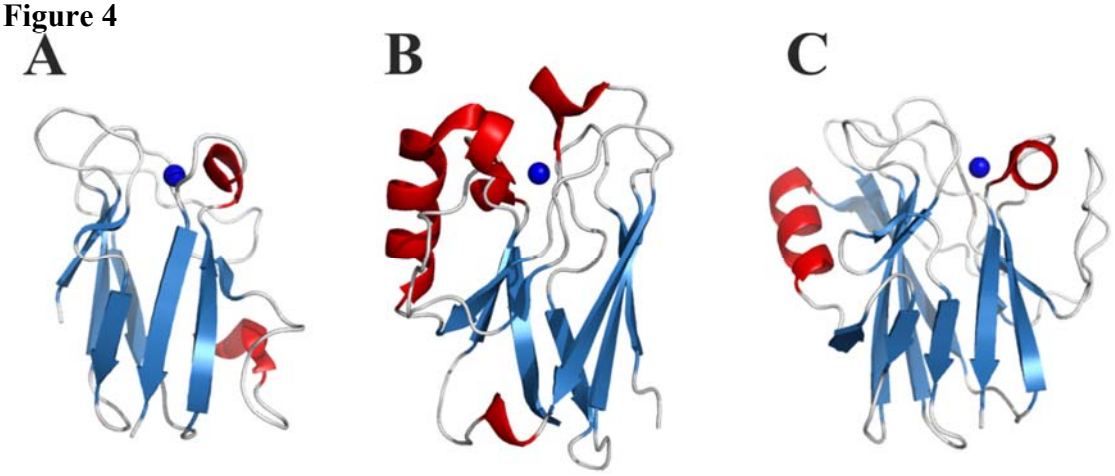

Figure 5

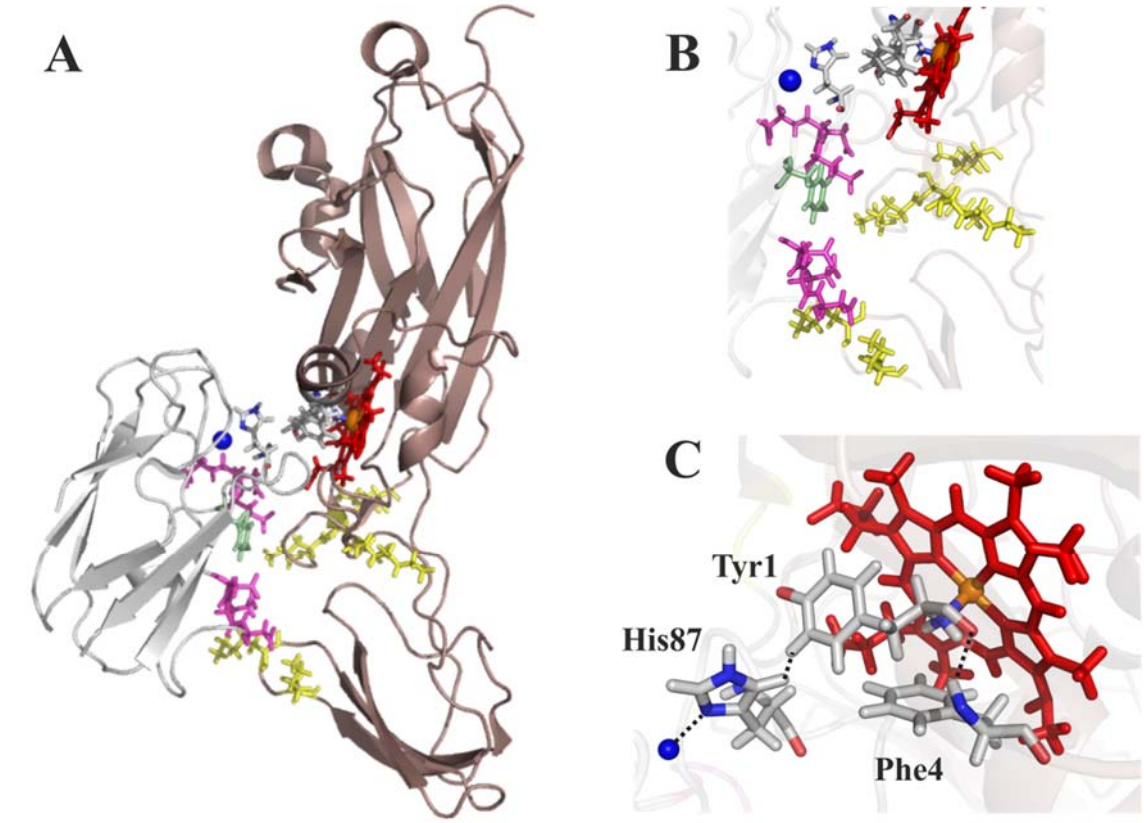

Figure 6

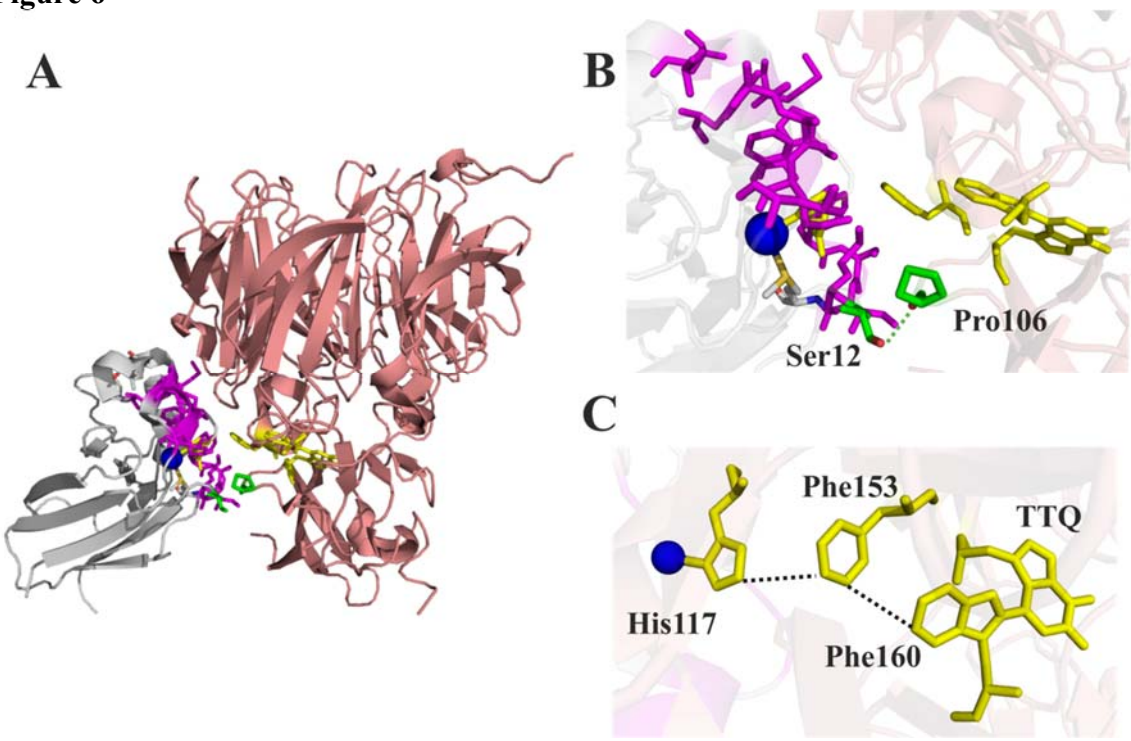

Figure 7

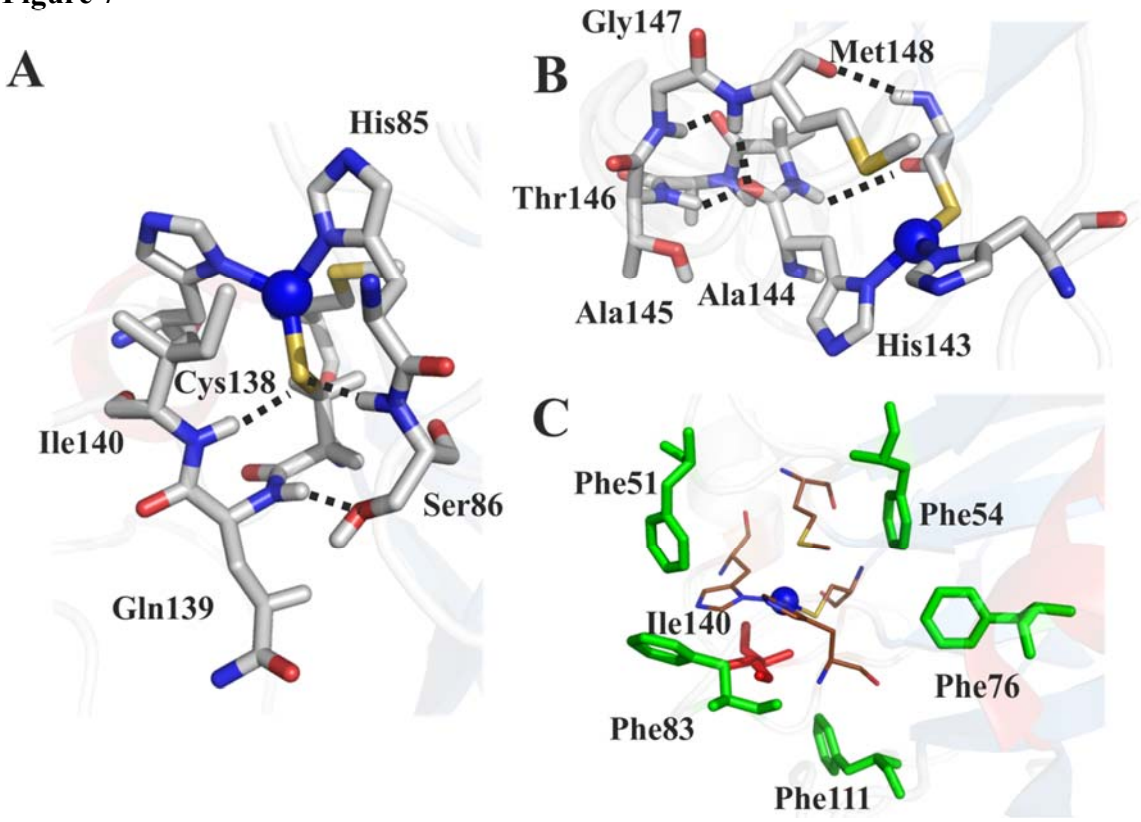
A
His85
Cys138
Ile140
Ser86
Gln139
B
Gly147
Met148
Thr146
Ala145
Ala144
His143
C
Phe51
Phe54
Ile140
Phe76
Phe83
Phe111

Figure 8

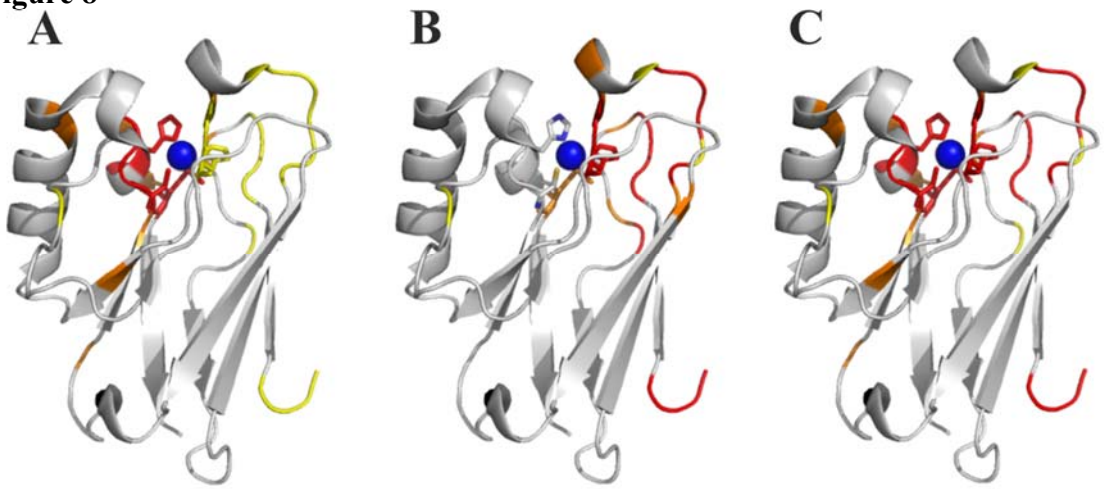

Figure 9

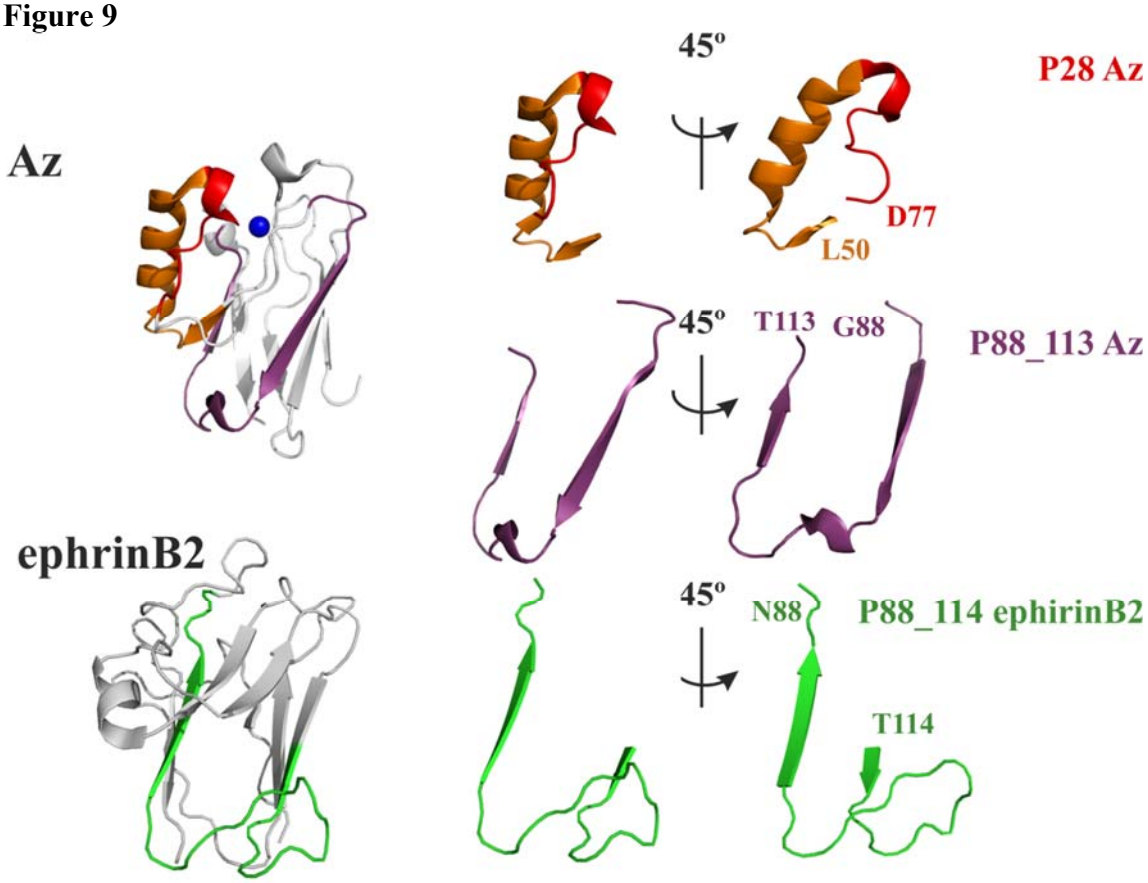
Az
ephrinB2
45°
P28 Az
D77
L50
45°
T113
G88
P88_113 Az
45°
N88
P88_114 ephirinB2
T114

Schemes

Scheme 1. Thermodynamic cycle that relates the redox potential of copper rusticyanin (step 1) with the copper(II) release (step 3) and copper(I) uptake (step 4) processes for the apoprotein and the redox potential of the free copper ion (step 2). This cycle is valid either for the folded or for the unfolded protein (from reference [103]). Gibs free energy values (in kcal/mol) for processes 1 to 4 are given as well.. Values given for processes 3 and 4 are referred to the corresponding equilibria in the sense of copper uptake, i.e., from the apo to the holoforms. A positive value means larger stability for the formation of the reduced holoprotein. Left values, marked with an F, (steps 1, 3, 4) refer to the processes for the folded form; right values (marked with the letter U)correspond to thos of the unfolded forms. In step 4, upper ΔG values correspond to the process 4, while lower ΔG parameters indicate the difference between the steps 4 and 3. Data obtained from reference [103].

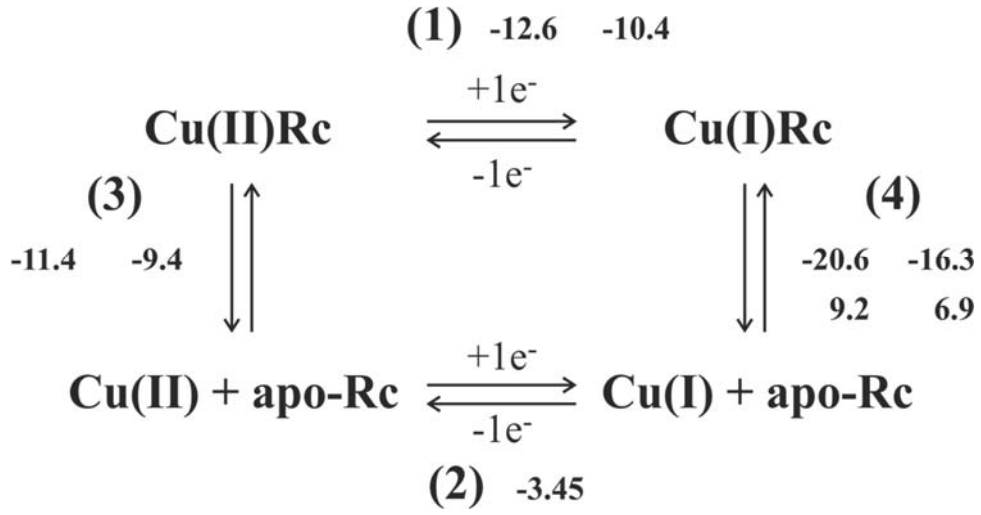

References

[1] S. Chan, B. Gerson, S. Subramaniam, Clin. Lab. Med. 18 (1998) 673-685.

[2] A. Leone, J. F. B. Mercer Copper transport and its disorders: Molecular and cellular aspects New York, (1999) Vol. 448.

[3] D. L. de Romana, M. Olivares, R. Uauy, M. Araya, J. Trace Elem. Med. Biol. 25 (2011) 3-13.

[4] J. F. Riordan, B. L. Vallee, Adv. Exp. Med. Biol. 48 (1974) 33-57.

[5] R. R. Crichton, J. L. Pierre, Biometals 14 (2001) 99-112.

[6] H. B. Gray, B. G. Malmstrom, R. J. Williams, J. Biol. Inorg. Chem. 5 (2000) 551-559.

[7] B. E. Ramirez, B. G. Malmstrom, J. R. Winkler, H. B. Gray, Proc. Natl. Acad. Sci. U.S.A. 92 (1995) 11949-11951.

[8] E. I. Solomon, X. Xie, A. Dey, Chem. Soc. Rev. 37 (2008) 623-638.

[9] I. Bertini, C. O. Fernandez, B. G. Karlson, J. Leckner, C. Luchinat, B. G. Malmström, A. M. Nersissian, R. Pierattelli, E. Shipp, J. Valentine, S., A. J. Vila, J. Am. Chem. Soc. 122 (2000) 3701-3707.

[10] A. M. Nersissian, E. L. Shipp (2002) in Adv. Protein. Chem., 271-340, Academic Press, San Diego.

[11] I. S. MacPherson, M. E. Murphy, Cell. Mol. Life Sci. 64 (2007) 2887-2899.

[12] L. M. Gaetke, H. S. Chow-Johnson, C. K. Chow, Arch. Toxicol. 88 (2014) 1929-1938.

[13] D. R. Brown, K. Qin, J. W. Herms, A. Madlung, J. Manson, R. Strome, P. E. Fraser, T. Kruck, A. von Bohlen, W. Schulz-Schaeffer, A. Giese, D. Westaway, H. Kretzschmar, Nature 390 (1997) 684-687.

[14] M. Patil, K. A. Sheth, A. C. Krishnamurthy, H. Devarbhavi, J. Clin. Exp. Hepatol. 3 (2013) 321-336.

[15] M. C. Miotto, E. E. Rodriguez, A. A. Valiente-Gabioud, V. Torres-Monserrat, A. Binolfi, L. Quintanar, M. Zweckstetter, C. Griesinger, C. O. Fernandez, Inorg. Chem. 53 (2014) 4350-4358.

[16] S. Montes, S. Rivera-Mancia, A. Diaz-Ruiz, L. Tristan-Lopez, C. Rios, Oxid. Med.Cell. Longev. (2014) 147251.

[17] A. I. Bush, J Alzheimers Dis 33 (2013) S277-281.

[18] C. Kaintz, S. G. Mauracher, A. Rompel, Adv. Protein Chem. Struct. Biol 97 (2014) 1-35.

[19] S. M. Jones, E. I. Solomon, Cell. Mol. Life Sci. 72 (2015) 869-883.

[20] P. Wittung-Stafshede, E. Gomez, A. Ohman, R. Aasa, R. M. Villahermosa, J. Leckner, B. G. Karlsson, D. Sanders, J. A. Fee, J. R. Winkler, B. G. Malmstrom, H. B. Gray, M. G. Hill, Biochim. Biophys. Acta 1388 (1998) 437-443.

[21] D. W. Randall, D. R. Gamelin, L. B. LaCroix, E. I. Solomon, J. Biol. Inorg. Chem. 5 (2000) 16-19.

[22] S. I. Gorelsky, X. Xie, Y. Chen, J. A. Fee, E. I. Solomon, J. Am. Chem. Soc. 128 (2006) 16452-16453.

[23] F. Neese, W. G. Zumft, W. E. a. Antholine, P. M. H. Kroneck, J.Am.Chem.Soc. 118 (1996) 8692-8699.

[24] O. Einarsdottir, W. McDonald, C. Funatogawa, I. Szundi, W. H. Woodruff, R. B. Dyer, Biochim.Biophys. Acta 1847 (2015) 109-118.

[25] S. Papa, N. Capitanio, G. Villani, G. Capitanio, A. Bizzoca, L. L. Palese, V. Carlino, E. De Nitto, Biochimie 80 (1998) 821-836.

[26] S. Dell'Acqua, S. R. Pauleta, I. Moura, J. J. Moura, J. Biol.Inorg. Chem. 16 (2011) 183-194.

[27] R. L. Lieberman, D. M. Arciero, A. B. Hooper, A. C. Rosenzweig, Biochemistry 40 (2001) 5674-5681.

[28] L. Basumallick, R. Sarangi, S. DeBeer George, B. Elmore, A. B. Hooper, B. Hedman, K. O. Hodgson, E. I. Solomon, J. Am. Chem. Soc. 127 (2005) 3531-3544.

[29] E. I. Solomon, D. E. Heppner, E. M. Johnston, J. W. Ginsbach, J. Cirera, M. Qayyum, M. T. Kieber-Emmons, C. H. Kjaergaard, R. G. Hadt, L. Tian, Chem. Rev. 114 (2014) 3659-3853.

[30] A. J. Vila, FEBS Lett. 355 (1994) 15-18.

[31] P. J. Hart, A. M. Nersissian, R. G. Herrmann, R. M. Nalbandyan, J. S. Valentine, D. Eisenberg, Protein Sci. 5 (1996) 2175-2183.

[32] K. M. Lancaster, S. DeBeer George, K. Yokoyama, J. H. Richards, H. B. Gray, Nat. Chem. 1 (2009) 711-715.

[33] H. B. Gray, E. I. Solomon (1981) in Copper Proteins, 1-39, Wiley, New York.

[34] R. G. Hadt, S. I. Gorelsky, E. I. Solomon, J. Am. Chem. Soc. 136 (2014) 15034-15045.

[35] E. I. Solomon, K. W. Penfield, A. A. Geweirth, M. D. Lowery, S. E. Shadle, G. A. Guckert, L. B. LaCroix, Inorg.Chim.Acta 243 (1996) 67-78.

[36] R. K. Szilagyi, E. I. Solomon, Curr.Opin.Chem. Biol 6 (2002) 250-258.

[37] R. Langen, I. J. Chang, J. P. Germanas, J. H. Richards, J. R. Winkler, H. B. Gray, Science 268 (1995) 1733-1735.

[38] M. C. Machczynski, H. B. Gray, J. H. Richards, J. Inorg.Biochem.88 (2002) 375-380.

[39] I. Diaz-Moreno, A. Diaz-Quintana, M. A. De la Rosa, M. Ubbink, J. Biol. Chem. 280 (2005) 18908-18915.

[40] F. P. Molina-Heredia, J. Wastl, J. A. Navarro, D. S. Bendall, M. Hervas, C. J. Howe, M. A. De La Rosa, Nature 424 (2003) 33-34.

[41] E. L. Gross, Photosynth. Res. 37 (1993) 103-116.

[42] C. Buning, G. W. Canters, P. Comba, C. Dennison, L. Jeuken, M. Melter, J. Sanders-Loehr, J. Am. Chem. Soc. 122 (2000) 204-211.

[43] A. Donaire, B. Jimenez, C. O. Fernandez, R. Pierattelli, T. Niizeki, J. M. Moratal, J. F. Hall, T. Kohzuma, S. S. Hasnain, A. J. Vila, J. Am. Chem. Soc. 124 (2002) 13698-13708.

[44] J. J. Warren, M. E. Ener, A. Vlcek, Jr., J. R. Winkler, H. B. Gray, Coord. Chem. Rev. 256 (2012) 2478-2487.

[45] F. Cutruzzola, M. Arese, G. Ranghino, G. van Pouderoyen, G. Canters, M. Brunori, J. Inorg. Biochem. 88 (2002) 353-361.

[46] C. Lange, T. Cornvik, I. Diaz-Moreno, M. Ubbink, Biochim. Biophys. Acta 1707 (2005) 179-188.

[47] A. B. Hope, Biochim. Biophys. Acta 1456 (2000) 5-26.

[48] H. Yang, J. Liu, X. Wen, C. Lu, Biochim. Biophys.Acta 1847 (2015) 838-848.

[49] S. Dell'acqua, I. Moura, J. J. Moura, S. R. Pauleta, J. Biol.Inorg. Chem. 16 (2011) 1241-1254.

[50] N. Sukumar, Z. W. Chen, D. Ferrari, A. Merli, G. L. Rossi, H. D. Bellamy, A. Chistoserdov, V. L. Davidson, F. S. Mathews, Biochemistry 45 (2006) 13500-13510.

[51] R. A. Marcus, N. Sutin, Biochim.Biophys.Acta 811 (1985) 265-275.

[52] R. Marcus, J.Chem.Phys. 43 (1965) 2654-2654.

[53] S. Wherland, R. A. Holwerda, R. C. Rosenberg, H. B. Gray, J. Am. Chem. Soc. 97 (1975) 5260-5262.

[54] K. C. Cho, D. F. Blair, U. Banerjee, J. J. Hopfield, H. B. Gray, I. Pecht, S. I. Chan, Biochemistry 23 (1984) 1858-1862.

[55] R. Margalit, N. M. Kostic, C. M. Che, D. F. Blair, H. J. Chiang, I. Pecht, J. B. Shelton, J. R. Shelton, W. A. Schroeder, H. B. Gray, Proc. Natl. Acad. Sci. U.S.A. 81 (1984) 6554-6558.

[56] M. Goldberg, I. Pecht, Isr. J. Med. Sci. 11 (1975) 1182.

[57] M. Faraggi, I. Pecht, Biochem.Biophys. Res. Commun. 45 (1971) 842-848.

[58] C. Dennison, Nat.Prod. Rep. 25 (2008) 15-24.

[59] S. Yanagisawa, C. Dennison, J. Am. Chem. Soc. 125 (2003) 4974-4975.

[60] M. Hay, J. H. Richards, Y. Lu, Proc. Natl. Acad. Sci. U.S.A 93 (1996) 461-464.

[61] A. Romero, C. W. Hoitink, H. Nar, R. Huber, A. Messerschmidt, G. W. Canters, J. Mol. Biol. 229 (1993) 1007-1021.

[62] K. M. Clark, Y. Yu, N. M. Marshall, N. A. Sieracki, M. J. Nilges, N. J. Blackburn, W. A. van der Donk, Y. Lu, J. Am. Chem. Soc. 132 (2010) 10093-10101.

[63] M. E. Palm-Espling, M. S. Niemiec, P. Wittung-Stafshede, Biochim. Biophys. Acta 1823 (2012) 1594-1603.

[64] I. Pozdnyakova, P. Wittung-Stafshede, J. Am. Chem. Soc. 123 (2001) 10135-10136.

[65] D. Milardi, D. M. Grasso, M. P. Verbeet, G. W. Canters, C. La Rosa, Arch. Biochem. Biophys. 414 (2003) 121-127.

[66] L. A. Alcaraz, A. Donaire, FEBS Lett. 579 (2005) 5223-5226.

[67] C. Romero, J. M. Moratal, A. Donaire, FEBS Lett. 440 (1998) 93-98.

[68] C. Li, K. Sato, S. Monari, I. Salard, M. Sola, M. J. Banfield, C. Dennison, Inorg. Chem. 50 (2011) 482-488.

[69] G. Battistuzzi, M. Borsari, G. W. Canters, G. di Rocco, E. de Waal, Y. Arendsen, A. Leonardi, A. Ranieri, M. Sola, Biochemistry 44 (2005) 9944-9949.

[70] R. C. n. Blake, E. A. Shute, Biochemistry 33 (1994) 9220-9228.

[71] T. Yamanaka, Y. Fukumori, FEMS Microbiol Rev 17 (1995) 401-413.

[72] A. Amouric, C. Brochier-Armanet, D. B. Johnson, V. Bonnefoy, K. B. Hallberg, Microbiology 157 (2011) 111-122.

[73] B. Jiménez, M. Piccioli, J. M. Moratal, A. Donaire, Biochemistry 42 (2003) 10396-10405.

[74] J. G. Grossmann, J. F. Hall, L. D. Kanbi, S. S. Hasnain, Biochemistry 41 (2002) 3613-3619.

[75] A. Donaire, B. Jiménez, J. M. Moratal, J. F. Hall, S. S. Hasnain, Biochemistry 40 (2001) 837-846.

[76] M. H. Olsson, G. Hong, A. Warshel, J. Am. Chem. Soc. 125 (2003) 5025-5039.

[77] B. P. Mukhopadhyay, B. Ghosh, H. R. Bairagya, T. K. Nandi, B. Chakrabarti, A. K. Bera, J. Biomol. Struct. Dyn. 25 (2008) 543-551.

[78] B. P. Mukhopadhyay, B. Ghosh, H. R. Bairagya, A. K. Bera, T. K. Nandi, S. B. Das, J. Biomol.Struct. Dyn. 25 (2007) 157-164.

[79] M. Choi, V. L. Davidson, Metallomics 3 (2011) 140-151.

[80] Z. X. Xia, W. W. Dai, Y. N. He, S. A. White, F. S. Mathews, V. L. Davidson, J. Biol. Inorg. Chem. 8 (2003) 843-854.

[81] L. Chen, R. C. Durley, F. S. Mathews, V. L. Davidson, Science 264 (1994) 86-90.

[82] R. Remenyi, L. J. Jeuken, P. Comba, G. W. Canters, JBIC 6 (2001) 23-26.

[83] A. R. Pearson, R. Pahl, E. G. Kovaleva, V. L. Davidson, C. M. Wilmot, J. Synchrotron Radiat. 14 (2007) 92-98.

[84] K. H. Tang, K. Barry, O. Chertkov, E. Dalin, C. S. Han, L. J. Hauser, B. M. Honchak, L. E. Karbach, M. L. Land, A. Lapidus, F. W. Larimer, N. Mikhailova, S. Pitluck, B. K. Pierson, R. E. Blankenship, BMC Genomics 12 (2011) 334.

[85] J. D. King, L. Harrington, B. M. Lada, G. He, J. W. Cooley, R. E. Blankenship, Arch. Biochem. Biophys. 564 (2014) 237-243.

[86] B. Scharf, M. Engelhard, Biochemistry 32 (1993) 12894-12900.

[87] B. Scharf, R. Wittenberg, M. Engelhard, Biochemistry 36 (1997) 4471-4479.

[88] I. V. Pearson, M. D. Page, R. J. van Spanning, S. J. Ferguson, J. Bacteriol. 185 (2003) 6308-6315.

[89] P. Gast, F. G. Broeren, S. Sottini, R. Aoki, A. Takashina, T. Yamaguchi, T. Kohzuma, E. J. Groenen, J. Inorg. Biochem. 137 (2014) 57-63.

[90] C. A. Libeu, M. Kukimoto, M. Nishiyama, S. Horinouchi, E. T. Adman, Biochemistry 36 (1997) 13160-13179.

[91] A. M. Nersissian, C. Immoos, M. G. Hill, P. J. Hart, G. Williams, R. G. Herrmann, J. S. Valentine, Protein Sci 7 (1998) 1915-1929.

[92] J. Dong, S. T. Kim, E. M. Lord, Plant. Physiol. 138 (2005) 778-789.

[93] O. Einsle, Z. Mehrabian, R. Nalbandyan, A. Messerschmidt, J. Biol. Inorg. Chem. 5 (2000) 666-672.

[94] J. A. Kreps, Y. Wu, H. S. Chang, T. Zhu, X. Wang, J. F. Harper, Plant Physiol 130 (2002) 2129-2141.

[95] M. Fedorova, J. van de Mortel, P. A. Matsumoto, J. Cho, C. D. Town, K. A. VandenBosch, J. S. Gantt, C. P. Vance, Plant.Physiol. 130 (2002) 519-537.

[96] B. G. Malmström, Eur. J. Biochem. 223 (1994) 711-718.

[97] B. G. Malmström, Z. Naturwiss. Med. Grundlagenforsch 2 (1965) 259-266.

[98] B. L. Vallee, R. J. P. Williams, Proc. Natl. Acad. Sci. U.S.A. 59 (1968) 498-505.

[99] U. Ryde, M. H. Olsson, B. O. Roos, J. O. De Kerpel, K. Pierloot, J. Biol.Inorg. Chem. 5 (2000) 565-574.

[100] U. Ryde, M. H. Olsson, K. Pierloot, B. O. Roos, J. Mol.Biol. 261 (1996) 586-596.

[101] L. A. Abriata, A. J. Vila, M. Dal Peraro, J. Biol.Inorg. Chem. 19 (2014) 565-575.

[102] L. A. Alcaraz, B. Jiménez, J. M. Moratal, A. Donaire, Prot. Sci. 14 (2005) 1710-1722.

[103] L. A. Alcaraz, J. Gomez, P. Ramirez, J. J. Calvente, R. Andreu, A. Donaire, Bioinorg. Chem.Appl. (2007) 54232.

[104] J. Marks, I. Pozdnyakova, J. Guidry, P. Wittung-Stafshede, J. Biol. Inorg. Chem. 9 (2004) 281-288.

[105] M. J. Feio, A. Diaz-Quintana, J. A. Navarro, M. A. De la Rosa, Biochemistry 45 (2006) 4900-4906.

[106] G. A. Guckert, M. D. Lowery, E. I. Solomon, J.Am.Chem.Soc. 117 (1995) 2817-2844.

[107] N. M. Marshall, D. K. Garner, T. D. Wilson, Y. G. Gao, H. Robinson, M. J. Nilges, Y. Lu, Nature 462 (2009) 113-116.

[108] J. J. Warren, J. H. Lancaster, H. B. Richards, H. B. Gray, J. Inorg. Biochem. 115 (2012) 119-126.

[109] R. E. Diederix, G. W. Canters, C. Dennison, Biochemistry 39 (2000) 9551-9560.

[110] J. F. Hall, L. D. Kanbi, R. W. Strange, S. S. Hasnain, Biochemistry 38 (1999) 12675-12680.

[111] L. D. Kanbi, S. Antonyuk, M. A. Hough, J. F. Hall, F. E. Dodd, S. S. Hasnain, J.Mol.Biol. 320 (2002) 263-275.

[112] T. E. Machonkin, H. H. Zhang, B. Hedman, K. O. Hodgson, E. I. Solomon, Biochemistry 37 (1998) 9570-9578.

[113] M. L. Barrett, I. Harvey, M. Sundararajan, R. Surendran, J. F. Hall, M. J. Ellis, M. A. Hough, R. W. Strange, I. H. Hillier, S. S. Hasnain, Biochemistry 45 (2006) 2927-2939.

[114] L. J. Jeuken, M. Ubbink, J. H. Bitter, P. van Vliet, W. Meyer-Klaucke, G. W. Canters, J. Mol. Biol. 299 (2000) 737-755.

[115] T. den Blaauwen, C. W. Hoitink, G. W. Canters, J. Han, T. M. Loehr, J. Sanders-Loehr, Biochemistry 32 (1993) 12455-12464.

[116] J. F. Hall, L. D. Kanbi, I. Harvey, L. M. M. Murphy, S. S. Hasnain, Biochemistry 37 (1998) 11451-11458.

[117] M. T. Giudici-Orticoni, F. Guerlesquin, M. Bruschi, W. Nitschke, J.Biol.Chem. 274 (1999) 30365-30369.

[118] J. J. Regan, A. J. Di Bilio, R. Langen, L. K. Skov, J. R. Winkler, H. B. Gray, J. N. Onuchic, Chem. Biol. 2 (1995) 489-496.

[119] J. R. Winkler, P. Wittung-Stafshede, J. Leckner, B. G. Malmstrom, H. B. Gray, Proc. Natl. Acad. Sci. U.S.A. 94 (1997) 4246-4249.

[120] A. J. Di Bilio, M. G. Hill, N. Bonander, B. G. Karlson, R. M. Villahermosa, B. G. Malmström, J. R. Winkler, H. B. Gray, J.Am.Chem.Soc. 119 (1997) 9921-9922.

[121] O. Farver, N. M. Marshall, S. Wherland, Y. Lu, I. Pecht, Proc. Natl. Acad. Sci. U.S.A. 110 (2013) 10536-10540.

[122] D. Sun, X. Li, F. S. Mathews, V. L. Davidson, Biochemistry 44 (2005) 7200-7206.

[123] H. Nar, A. Messerschmidt, R. Huber, M. v. Kamp, G. W. Canters, FEBS Lett. 306 (1992) 119.

[124] W. E. B. Shepard, R. L. Kingston, B. F. Anderson, E. N. Baker, Acta Cryst.D D49 (1993) 331.

[125] T. P. J. Garrett, D. J. Clingeleffer, J. M. Guss, S. J. Rogers, H. C. Freeman, J.Biol.Chem. 259 (1984) 2822.

[126] K. Petratos, M. Papadovasilaki, Z. Dauter, FEBS Lett 368 (1995) 432-434.

[127] R. Durley, L. Chen, L. W. Lim, F. S. Mathews, V. L. Davidson, Protein Sci 2 (1993) 739-752.

[128] N. J. Robinson, D. R. Winge, Annu. Rev. Biochem. 79 (2010) 537-562.

[129] D. L. Huffman, T. V. O'Halloran, Annu.Rev. Biochem. 70 (2001) 677-701.

[130] L. Banci, I. Bertini, F. Cantini, I. C. Felli, L. Gonnelli, N. Hadjiliadis, R. Pierattelli, A. Rosato, P. Voulgaris, Nat. Chem. Biol. 2 (2006) 367-368.

[131] C. E. Blaby-Haas, T. Padilla-Benavides, R. Stube, J. M. Arguello, S. S. Merchant, Proc. Natl. Acad. Sci. U.S.A 111 (2014) E5480-5487.

[132] S. Tottey, P. R. Rich, S. A. Rondet, N. J. Robinson, J. Biol. Chem. 276 (2001) 19999-20004.

[133] L. A. Abriata, L. Banci, I. Bertini, S. Ciofi-Baffoni, P. Gkazonis, G. A. Spyroulias, A. J. Vila, S. Wang, Nat. Chem. Biol. 4 (2008) 599-601.

[134] J. M. Arguello, D. Raimunda, T. Padilla-Benavides, Front Cell. Infect.Microbiol. 3 (2013) 73.

[135] M. E. Zaballa, L. A. Abriata, A. Donaire, A. J. Vila, Proc.Natl. Acad. Sci. U.S.A 109 (2012) 9254-9259.

[136] S. Spreckelmeyer, C. Orvig, A. Casini, Molecules 19 (2014) 15584-15610.

[137] O. Silva Dde, Anticancer Agents Med. Chem. 10 (2010) 312-323.

[138] A. Alama, B. Tasso, F. Novelli, F. Sparatore, Drug. Discov. Today 14 (2009) 500-508.

[139] G. S. Yellol, A. Donaire, J. G. Yellol, V. Vasylyeva, C. Janiak, J. Ruiz, Chem. Commun. 49 (2013) 11533-11535.

[140] N. Bernardes, A. M. Chakrabarty, A. M. Fialho, Appl. Microbiol. Biotechnol. 97 (2013) 5189-5199.

[141] A. M. Chakrabarty, Adv. Exp. Med.Biol. 808 (2014) 41-49.

[142] N. Bernardes, A. S. Ribeiro, S. Abreu, A. F. Vieira, L. Carreto, M. Santos, R. Seruca, J. Paredes, A. M. Fialho, Int. J. Biochem. Cell. Biol. 50 (2014) 1-9.

[143] T. Yamada, Y. Hiraoka, M. Ikehata, K. Kimbara, B. S. Avner, T. K. Das Gupta, A. M. Chakrabarty, Proc. Natl. Acad. Sci. U.S.A 101 (2004) 4770-4775.

[144] A. Chaudhari, M. Mahfouz, A. M. Fialho, T. Yamada, A. T. Granja, Y. Zhu, W. Hashimoto, B. Schlarb-Ridley, W. Cho, T. K. Das Gupta, A. M. Chakrabarty, Biochemistry 46 (2007) 1799-1810.

[145] B. N. Taylor, R. R. Mehta, T. Yamada, F. Lekmine, K. Christov, A. M. Chakrabarty, A. Green, L. Bratescu, A. Shilkaitis, C. W. Beattie, T. K. Das Gupta, Cancer Res. 69 (2009) 537-546.

[146] T. Yamada, R. R. Mehta, F. Lekmine, K. Christov, M. L. King, D. Majumdar, A. Shilkaitis, A. Green, L. Bratescu, C. W. Beattie, T. K. Das Gupta, Mol. Cancer Ther. 8 (2009) 2947-2958.

[147] T. Yamada, K. Christov, A. Shilkaitis, L. Bratescu, A. Green, S. Santini, A. R. Bizzarri, S. Cannistraro, T. K. Gupta, C. W. Beattie, Br. J. Cancer 108 (2013) 2495-2504.

[148] T. Yamada, K. Christov, D. G. T.K., J. Clin. Oncol. 29 (2011) abstr e13513.

[149] R. R. Mehta, T. Yamada, B. N. Taylor, K. Christov, M. L. King, D. Majumdar, F. Lekmine, C. Tiruppathi, A. Shilkaitis, L. Bratescu, A. Green, C. W. Beattie, T. K. Das Gupta, Angiogenesis 14 (2011) 355-369.

[150] T. Yamada, Y. Hiraoka, T. K. Das Gupta, A. M. Chakrabarty, Cell Cycle 3 (2004) 1182-1187.

[151] T. Yamada, A. M. Fialho, V. Punj, L. Bratescu, T. K. Gupta, A. M. Chakrabarty, Cell Microbiol.7 (2005) 1418-1431.

[152] A. M. Fialho, A. M. Chakrabarty, Recent.Pat. Anticancer Drug.Discov. 2 (2007) 224-234.

[153] I. Cruz-Gallardo, I. Diaz-Moreno, A. Diaz-Quintana, A. Donaire, A. Velazquez-Campoy, R. D. Curd, K. Rangachari, B. Birdsall, A. Ramos, A. A. Holder, M. A. De la Rosa, J. Biol. Chem. 288 (2013) 20896-20907.

[154] A. Chaudhari, A. M. Fialho, D. Ratner, P. Gupta, C. S. Hong, S. Kahali, T. Yamada, K. Haldar, S. Murphy, W. Cho, V. S. Chauhan, T. K. Das Gupta, A. M. Chakrabarty, Cell Cycle 5 (2006) 1642-1648.

[155] T. Tiefenbrunn, W. Liu, Y. Chen, V. Katritch, C. D. Stout, J. A. Fee, V. Cherezov, PLoS One 6 (2011) e22348.

[156] T. Tsukihara, K. Shimokata, Y. Katayama, H. Shimada, K. Muramoto, H. Aoyama, M. Mochizuki, K. Shinzawa-Itoh, E. Yamashita, M. Yao, Y. Ishimura, S. Yoshikawa, Proc. Natl. Acad. Sci. U.S.A 100 (2003) 15304-15309.

[157] K. Brown, K. Djinovic-Carugo, T. Haltia, I. Cabrito, M. Saraste, J. J. Moura, I. Moura, M. Tegoni, C. Cambillau, J. Biol. Chem. 275 (2000) 41133-41136.

[158] G. S. Kachalova, A. C. Shosheva, G. P. Bourenkov, A. A. Donchev, M. I. Dimitrov, H. D. Bartunik, J. Inorg. Biochem. 115 (2012) 174-181.

[159] M. Ubbink, M. Ejdeback, B. G. Karlsson, D. S. Bendall, Structure 6 (1998) 323-335.

[160] H. Nar, A. Messerschmidt, R. Huber, M. van de Kamp, G. W. Canters, J.Mol.Biol. 221 (1991) 765-772.

[161] J. P. Himanen, K. R. Rajashankar, M. Lackmann, C. A. Cowan, M. Henkemeyer, D. B. Nikolov, Nature 414 (2001) 933-938.